Oncogene (2006) 25, 4975–4985

www.nature.com/onc

ORIGINAL ARTICLE

Regulation of vimentin by SIP1 in human epithelial breast tumor cells

S Bindels[1], M Mestdagt[1], C Vandewalle[2], N Jacobs[3], L Volders[1], A Noël[1], F van Roy[2], G Berx[2], J-M Foidart[1] and C Gilles[1]

[1]Laboratory of Tumor and Developmental Biology, Center for Biomedical Integrated Genoproteomics, University of Liège, CHU Sart-Tilman, Liège, Belgium; [2]Department for Molecular Biomedical Research, VIB-Ghent University, Ghent (Zwijnaarde), Belgium and [3]Laboratory of Anatomopathology, Center for Biomedical Integrated Genoproteomics, University of Liège, CHU Sart-Tilman, Liège, Belgium

The expression of Smad interacting protein-1 (SIP1; ZEB2) and the *de novo* expression of vimentin are frequently involved in epithelial-to-mesenchymal transitions (EMTs) under both normal and pathological conditions. In the present study, we investigated the potential role of SIP1 in the regulation of vimentin during the EMT associated with breast tumor cell migration and invasion. Examining several breast tumor cell lines displaying various degrees of invasiveness, we found SIP1 and vimentin expression only in invasive cell lines. Also, using a model of cell migration with human mammary MCF10A cells, we showed that SIP1 is induced specifically in vimentin-positive migratory cells. Furthermore, transfection of SIP1 cDNA in MCF10A cells increased their vimentin expression both at the mRNA and protein levels and enhanced their migratory abilities in Boyden Chamber assays. Inversely, inhibition of SIP1 expression by RNAi strategies in BT-549 cells and MCF10A cells decreased vimentin expression. We also showed that SIP1 transfection did not activate the TOP-FLASH reporter system, suggesting that the β-catenin/TCF pathway is not implicated in the regulation of vimentin by SIP1. Our results therefore implicate SIP1 in the regulation of vimentin observed in the EMT associated with breast tumor cell migration, a pathway that may contribute to the metastatic progression of breast cancer.
Oncogene (2006) **25,** 4975–4985. doi:10.1038/sj.onc.1209511; published online 27 March 2006

Keywords: vimentin; SIP1; cell migration

Introduction

During their metastatic conversion, epithelial cells acquire the ability to invade the surrounding tissue and disseminate into secondary organs. There is mounting evidence that the acquisition of migratory and invasive properties by epithelial cells is associated with the gain of mesenchymal characteristics and the loss of epithelial features, a phenomenon referred to as epithelial-to-mesenchymal transition (EMT) (Savagner, 2001; Thiery, 2002; Gotzmann *et al*., 2004; Gilles *et al*., 2004).

A growing number of zinc-finger transcription factors has now been implicated in the regulation of EMT phenomena. Among them is SIP1 (Smad Interacting Protein-1) or ZEB2, a large zinc-finger protein that, together with δEF1, belongs to a small family of transcriptional repressors. It has originally been identified as a factor binding the Smad proteins, implicated in the signaling by TGF-β (Verschueren *et al*., 1999). The δEF1/ZEB family comprises two vertebrate prototypes (δEF1/ZEB1 and SIP1/ZEB2) characterized by two zinc-finger clusters separated by a homeodomain. The N-terminal and C-terminal zinc-finger clusters are made of four and three zinc fingers, respectively. Each zinc-finger cluster recognizes a CACCT motif on the DNA but the full-length SIP1 molecule has been shown to bind a bipartite element composed of one 5′-CACCT and one 5′-CACCTG sequence (Remacle *et al*., 1999; Verschueren *et al*., 1999). A mechanism by which SIP1 might contribute to EMT processes is through its ability to downregulate E-cadherin. Indeed, SIP1 has been shown to bind the E-cadherin promoter and to downregulate the expression of this cell adhesion protein (Comijn *et al*., 2001; van Grunsven *et al*., 2003). E-cadherin is a transmembrane glycoprotein that mediates homotypic cell–cell contacts between epithelial cells and, thereby, largely contributes to the cohesive architecture of normal epithelia. The cytoplasmic part of E-cadherin is associated with the actin cytoskeleton via its cytoplasmic binding partners, the catenins (α-, β- and γ- catenin). Under particular conditions, when β-catenin is not sequestered in the junctional E-cadherin complexes, it can translocate in the nucleus where it acts as a transcriptional coactivator through its binding with the members of the TCF/LEF-1 (T-cell factor/lymphoid enhancer factor) transcription factor family (Bienz, 2005). Downregulation of E-cadherin expression and reorganization of E-cadherin-based adhesion junctions are considered hallmarks of EMT processes and have

Correspondence: Dr C Gilles, Laboratory of Tumor and Developmental Biology, Liège University, CHU Sart-Tilman, Tour de Pathologie B23, B-4000 Liège, Belgium.
E-mail: cgilles@ulg.ac.be
Received 7 July 2005; revised 13 February 2006; accepted 15 February 2006; published online 27 March 2006

largely been implicated in EMT associated with the acquisition of a migratory/invasive phenotype by epithelial tumor cells (Comijn *et al*., 2001; Van Aken *et al*., 2001; Peinado *et al*., 2004).

Besides the disorganization of E-cadherin-based junctional complexes, the *de novo* expression of vimentin is also frequently associated with EMT processes and with the metastatic conversion of epithelial cells. Vimentin is a type-III intermediate filament normally expressed in cells of mesenchymal origin (Steinert and Roop, 1988). However, numerous data have now demonstrated that vimentin can also be expressed in epithelial cells when they become involved in physiological or pathological processes requiring epithelial cell migration. Vimentin has indeed been described in migratory epithelial cells involved in embryonic and organogenesis processes, in placentation, wound healing and tumor invasion (Ramaekers *et al*., 1983; Guarino, 1995; Gilles and Thompson, 1996; Gilles *et al*., 1999, 2003). Also, vimentin-specific antisense cDNA or oligonucleotide transfection in vimentin-expressing cell lines was shown to reduce their *in vitro* invasiveness or migration, strongly emphasizing a functional contribution of vimentin to epithelial cell invasion/migration (Hendrix *et al*., 1997; Gilles *et al*., 1999; Singh *et al*., 2003). Accordingly, impaired wound healing has been observed in vimentin knockout mice (Eckes *et al*., 1998, 2000). Furthermore, a direct or indirect interaction of vimentin with microfilaments and microtubules and more particularly with molecules such as plectin or integrins has been described (Svitkina *et al*., 1996; Maniotis *et al*., 1997; Homan *et al*., 1998; Goldman *et al*., 1999; Wu *et al*., 1999; Gonzales *et al*., 2001; Tsuruta and Jones, 2003; Helfand *et al*., 2004; Kreis *et al*., 2005). A role of vimentin in the mechanical transduction of signals from the cell surface to the nucleus and in the overall reorganization of the cytoskeleton associated with cell motility and migration has therefore been suggested (Hendrix *et al*., 1996; Gilles *et al*., 1999; Eckes *et al*., 2000; Helfand *et al*., 2004).

Because both SIP1 and vimentin expression are clearly associated with EMT events, we thus examined in the present study the implication of SIP1 in the induction of vimentin expression associated with epithelial cell migration and invasion. We also explored the potential role of the β-catenin/TCF pathway in this regulation.

Results

Vimentin expression correlates with SIP1 expression in migratory/invasive breast cell lines

In order to examine the relationship between SIP1 and vimentin, we first analysed their expression in two non-invasive (MCF-7, T47D) and three invasive (MDA-231, BT549, Hs578T) epithelial breast cancer cell lines. The invasive phenotype of these breast cancer cells, as assessed by modified Boyden chamber assays, as well as their vimentin and E-cadherin expression status have been characterized in previous studies which established a clear association between high invasive properties and EMT traits such as vimentin expression and lack of E-cadherin expression (Thompson *et al*., 1992; Sommers *et al*., 1994; Nawrocki *et al*., 2001). Examining SIP1 in this set of breast cell lines, we observed that invasive breast cancer cell lines showed both SIP1 and vimentin mRNA expression in contrast to non-invasive cells (Figure 1). SIP1 and vimentin mRNA expression was also analysed in primary airway human fibroblasts versus primary human differentiated epithelial cells. Cells isolated from airway tissues were used because of the possibility to obtain a clear epithelial differentiation, characterized by the presence of ciliated cells, when cultivated in appropriate culture conditions. In support of the results obtained with the tumor cell lines suggesting that the invasive cell lines have gained mesenchymal characteristics, a weak expression of vimentin and no detectable expression of SIP-1 was found in differentiated lung epithelial cells whereas both mRNA were strongly co-expressed in fibroblasts (Figure 1).

Next, we studied SIP1 expression in relation to vimentin expression in a migration assay that we had previously used to demonstrate the transient expression of vimentin during epithelial cell migration (Gilles *et al*., 1999, 2003). Briefly, in this migration assay, MCF10A human breast cells are plated at high density in a glass ring and migrate as an outgrowth after the removal of the ring. In this assay, vimentin expression has been shown to vary in relationship with the migratory status of the cells. Using video microscopy, we indeed previously demonstrated that the subpopulation of cells at the periphery of the outgrowth is involved in an orientated migration and undergoes an EMT process characterized by the *de novo* expression of vimentin and a relocalization of E-cadherin and β-catenin (Gilles *et al*., 1999, 2003). In contrast, the stationary cells in the

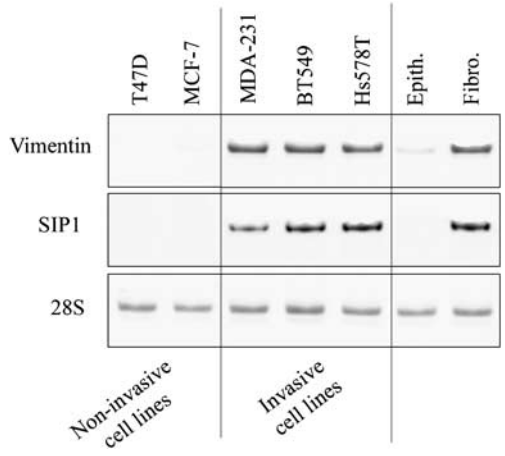

Figure 1 Expression of SIP1 correlates with vimentin expression in human breast cancer cell lines. RT–PCR analyses of vimentin and SIP1 were performed on five human tumor cell lines (T47D, MCF-7, MDA-231, BT549 and Hs578T) as well as in primary fibroblasts (Fibro.) and differentiated primary epithelial (Epith.) cells isolated from human airway tissues. 28S rRNA analysis is shown as control.

area initially delimited by the ring do not express vimentin and display a typical honeycomb pattern of E-cadherin and β-catenin staining. In the present study, we used two clones (#11 and #12) of MCF10A cells stably transfected with a plasmid containing the vimentin promoter controlling the expression of the enhanced green fluorescent protein (EGFP) gene (VP-EGFP MCF10A cells as previously described in Gilles *et al*., 1999). The VP-EGFP MCF10A cells were plated in the migration assays and sorted by FACS to physically separate the GFP-positive and the GFP-negative populations (Figure 2a). RT–PCR performed on these two separated cell populations clearly showed co-expression of SIP1 and vimentin mRNA in the migratory subpopulation (Figure 2b).

The effect of EGF on vimentin and SIP1 co-expression was also investigated in this assay. We indeed previously showed that EGF, which is present in the

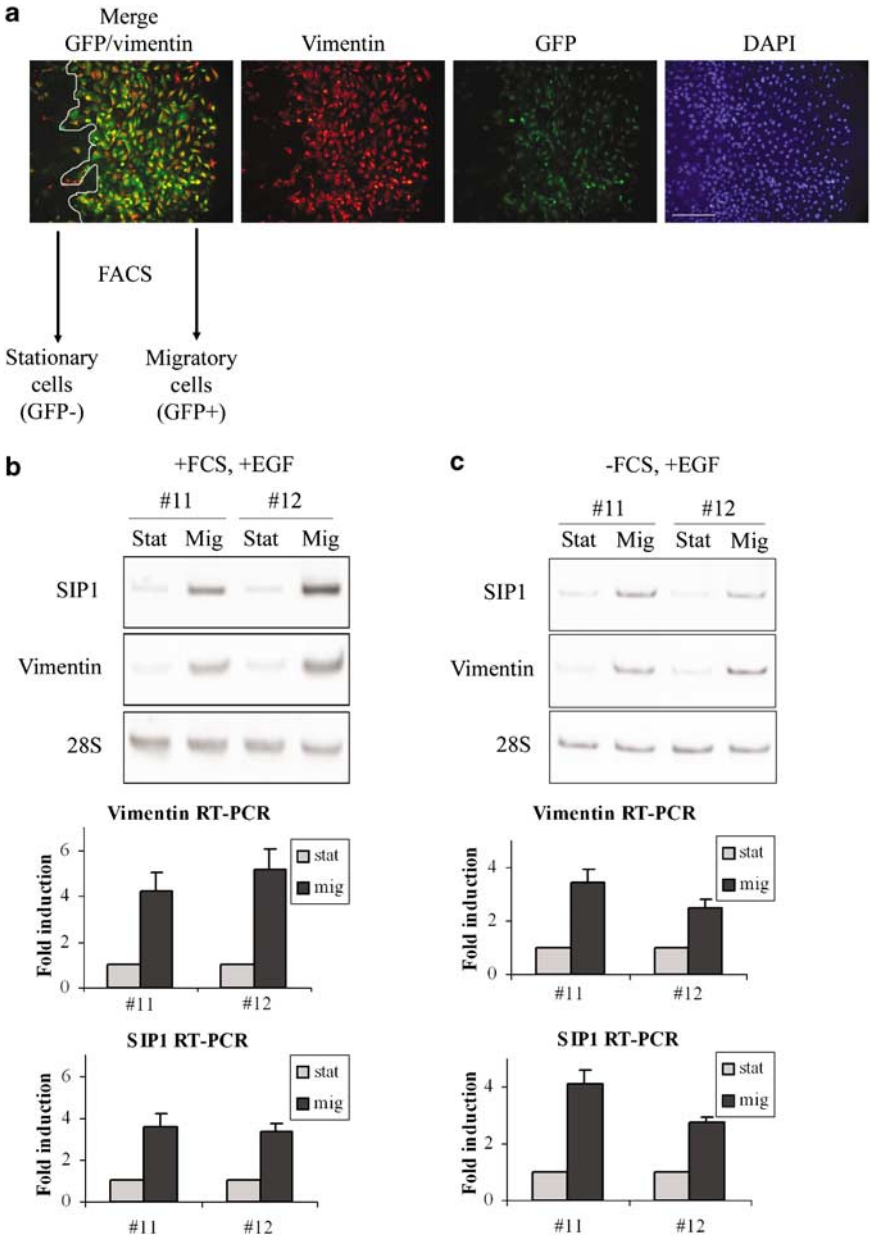

Figure 2 Expression of SIP1 correlates with vimentin expression in migratory MCF10A cells. (**a**) Single or double visualization (merge) of vimentin (in red) and EGFP expression driven by the vimentin promoter (in green) in VP-EGFP MCF10A cells plated in the migration assay. DAPI staining is in blue. The white line schematically represents the limit between the vimentin-positive and the vimentin-negative cell population. Bar = 80 μm. (**b**, **c**) RT–PCR analyses for SIP1 and vimentin were performed on migratory (mig) and stationary (stat) subpopulations sorted by FACS for GFP expression of two clones (#11 and #12) of VP-EGFP MCF10A plated in the migration assay in complete growth medium (FCS + EGF) (**b**) or in FCS-free, EGF-containing growth medium (**c**). 28S rRNA analysis is shown as control. Quantification of RT–PCR analyses of vimentin and SIP1 normalized for the 28S rRNA values in three independent migration and FACS sorting experiments, as described in (**b**, **c**), is shown. Data are expressed as fold induction in the migratory subpopulation relative to the stationary subpopulation ($P<0.05$).

growth medium of the MCF10A cells, induces vimentin expression in migratory MCF10A cells even in the absence of serum. Similar to our observations in the presence of complete growth medium (containing FCS and EGF) (Figure 2b), a strong co-expression of vimentin and SIP1 mRNA was also found in the migratory subpopulation of the two clones of VP-EGFP MCF10A plated in EGF-containing, serum-free medium (Figure 2c).

Smad interacting protein-1 regulates vimentin expression

Because of the correlation between vimentin and SIP1 expression in both the breast cancer cell line panel and the MCF10A migration assay, we examined whether SIP1 could regulate vimentin expression. We first observed that transient transfection of SIP1 cDNA for 24, 48 or 72 h clearly induced vimentin expression both at the mRNA (Figure 3a) and at the protein (Figure 3b) levels. This correlated with increased migratory properties in the Boyden chamber assay (Figure 3c).

Inversely, we investigated the effect of an inhibition of SIP1 on vimentin expression using RNAi strategies both on MCF10A cells and on vimentin-positive BT549 cells. Because an efficient diminution of SIP1 could not be achieved in MCF10A cells by transient transfection of SIP1 siRNA, these cells were transduced with two lentiviral constructs expressing two different SIP1 short hairpin RNA (shRNA) sequences which efficiently diminished SIP1 mRNA levels (Figure 4a). The SIP1 shRNA construct transduction also diminished vimentin expression both at the mRNA (60% decrease compared to control transduced cells) and at the protein level (Figure 4a and b). This was associated with a diminution of migratory properties in the Boyden chamber assay (Figure 4c). Strengthening these data obtained with MCF10A cells, we also showed that transient transfections of two species of SIP1 siRNA in vimentin-positive BT549 cells significantly decreased vimentin mRNA levels (34 and 28% decrease for siRNA 1 and 2, respectively) (Figure 5a). A decrease of vimentin protein expression was also observed (Figure 5b).

Because vimentin has been shown to be a target of the β-catenin/TCF pathway (Gilles *et al*., 2003) and because SIP1 has been described as a potent transcriptional repressor of E-cadherin (Comijn *et al*., 2001; van Grunsven *et al*., 2003), we examined whether the regulation of vimentin by SIP1 involved the β-catenin/TCF pathway. A downregulation of E-cadherin may indeed result in increased availability of β-catenin in the nucleus. We thus first confirmed that SIP1 and E-cadherin expression were inversely correlated in the breast tumor cell lines (Figure 6a). This was also seen in the MCF10A migration assay (Figure 6b). Furthermore, transfection of SIP1 cDNA in MCF10A cells decreased the level of E-cadherin mRNA in these cells (Figure 6c). In order to analyse the implication of the β-catenin/TCF pathway in SIP1-induced vimentin expression, we next examined the ability of SIP1 to transactivate a luciferase reporter plasmid containing wild-type (TOP-FLASH) or mutated (FOP-FLASH) β-catenin/TCF-binding sites as regulatory elements. Although SIP1 cDNA transfection clearly activated the vimentin promoter reporter

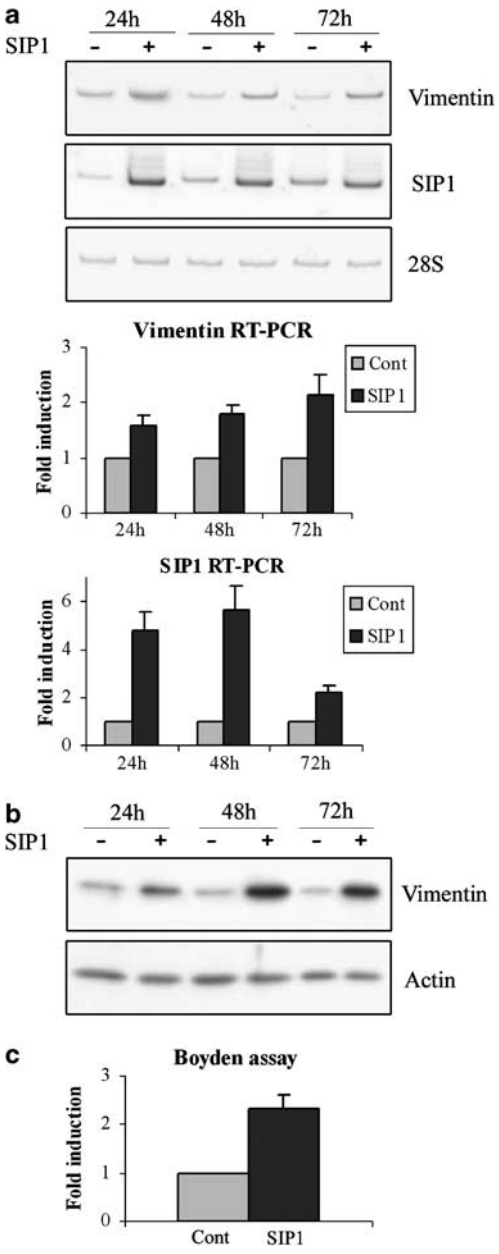

Figure 3 SIP1 transfection regulates vimentin expression. (**a**) RT–PCR analyses of vimentin and SIP1 expression in MCF10A cells transiently transfected with SIP1 cDNA for 24, 48 or 72 h. Quantification of RT–PCR analyses of vimentin, normalized for the 28S rRNA values, in three independent transfection experiments is shown. Data are expressed as fold induction in SIP1 transfectants relative to the backbone vector transfectants ($P<0.05$). (**b**) Western blotting analyses of vimentin expression in MCF10A cells transiently transfected with SIP1 cDNA for 24, 48 or 72 h. Actin detection is shown as a control. A representative experiment is shown out of three independent experiments performed. (**c**) Boyden chamber analyses of the migratory abilities of MCF10A transfected for 48 h with the SIP1 cDNA (SIP1) or the backbone vector (Cont). Data are expressed as fold induction for SIP1 transfectants relative to the backbone vector transfectants ($P<0.05$).

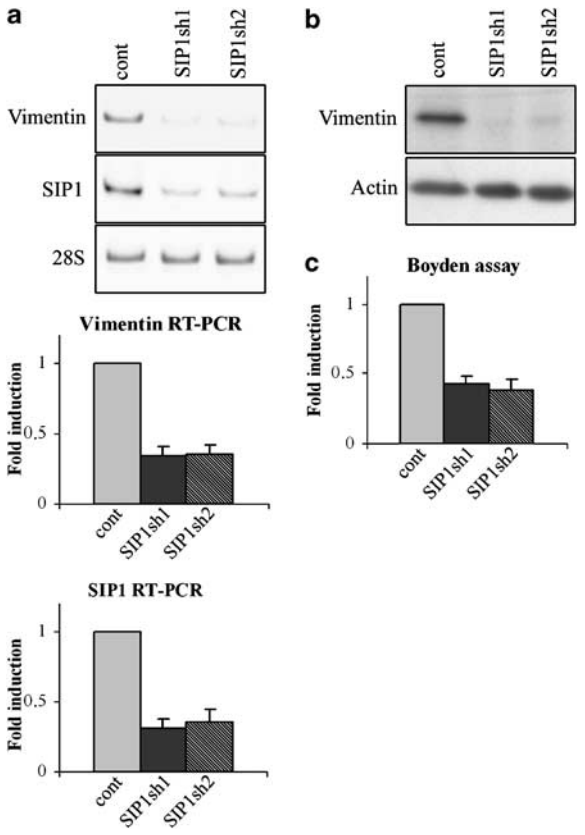

Figure 4 SIP1 shRNA decreased vimentin expression and migratory abilities of MCF10A cells. MCF10A cells were transduced with lentiviral constructs expressing two different sequences of SIP1 shRNA (SIP1sh1, SIP1sh2) or with a control vector (Cont). (**a**) RT–PCR analyses of vimentin and SIP1 in the SIP1 shRNA-expressing cells compared to the control cells. Quantification of RT–PCR analyses of vimentin normalized for the 28S rRNA values in three independent transfection experiments is shown. Data are expressed as fold induction in shRNA-expressing cells relative to the controls ($P<0.01$). (**b**) Western blot analyses of vimentin expression in SIP1 shRNA-expressing cells. Actin was used as a control. A representative experiment is shown out of three independent experiments performed. (**c**) Analyses of the migratory abilities of SIP1 shRNA-expressing MCF10A cells compared to control cells in the Boyden chamber assay. Data are expressed as fold induction for SIP1 shRNA-expressing cells relative to the control cells ($P<0.05$).

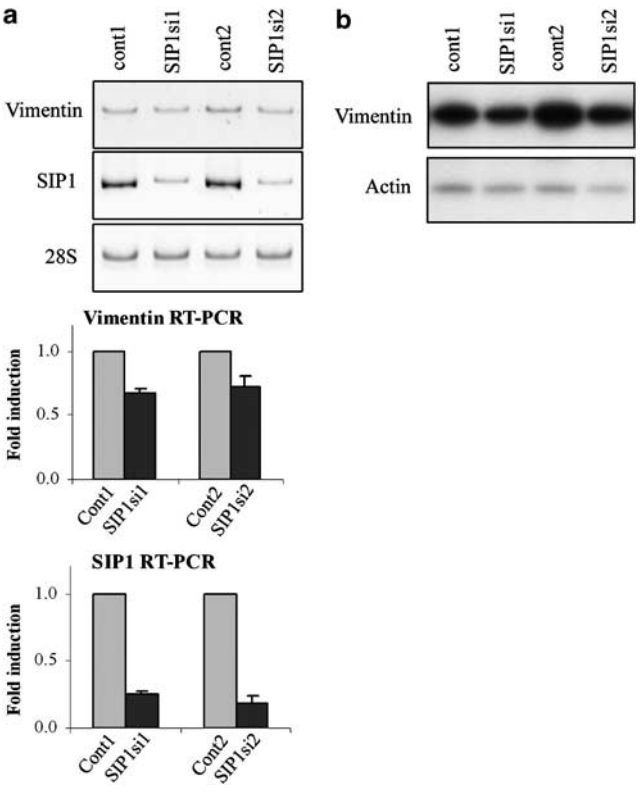

Figure 5 SIP1 siRNA decreased vimentin expression in BT-549 cells. BT549 cells were transfected with either two different siRNA sequences against SIP1 (SIPsi1, SIPsi2) or two control siRNAs (cont1 and cont2). (**a**) RT–PCR analyses of vimentin and SIP1 in the SIP1 siRNA-expressing cells compared to the control cells. Quantification of RT–PCR analyses of vimentin normalized for the 28S rRNA values in three independent transfection experiments is shown. Data are expressed as fold induction in SIP1 siRNA-expressing cells relative to the controls ($P<0.01$). (**b**) Western blot analyses of vimentin expression in SIP1 siRNA-expressing cells. Actin was used as a control. A representative experiment is shown out of three independent experiments performed.

construct (Figure 7a), it failed to activate the TOP-FLASH reporter system (Figure 7b). This suggests that SIP1 does not activate the β-catenin/TCF pathway. Accordingly, we did not observe any increase of β-catenin in the nuclear fraction (nor in the membranous or cytosolic fractions) of cells transfected with SIP1 cDNA though the presence of the myc-tagged SIP1 was detected (Figure 7c). Since it has been suggested that the NH_2-unphosphorylated form of β-catenin is mainly implicated in the transcriptional activity of β-catenin (Staal *et al*., 2002), we also examined this particular form of β-catenin. Using a specific antibody against the unphosphorylated β-catenin, we still did not observe any increase of this particular form in the nuclei of SIP1-transfected cells (data not shown).

Discussion

In the present study, we demonstrate that SIP1 regulates vimentin expression in epithelial cells and emphasize the implication of this regulation in epithelial breast cancer cell migration/invasion. We indeed show that (1) SIP1 expression coincided with vimentin expression in invasive breast tumor cell lines, (2) SIP1 and vimentin expression were specifically induced in migratory epithelial MCF10A cells, (3) SIP1 cDNA transfection increased vimentin expression and migratory abilities of MCF10A cells, (4) SIP1-specific siRNA or shRNA diminished vimentin expression in invasive breast tumor cell lines and (5) the activation of the vimentin promoter by SIP1 was not associated with the activation of the β-catenin/TCF/LEF signaling pathway.

Upon examination of several human breast cancer cell lines, we found a clear correlation between vimentin and SIP1 expression in invasive cell lines. A correlation between vimentin and SIP1 expression was also obvious in the assay of MCF10A cell migration. Previously, this

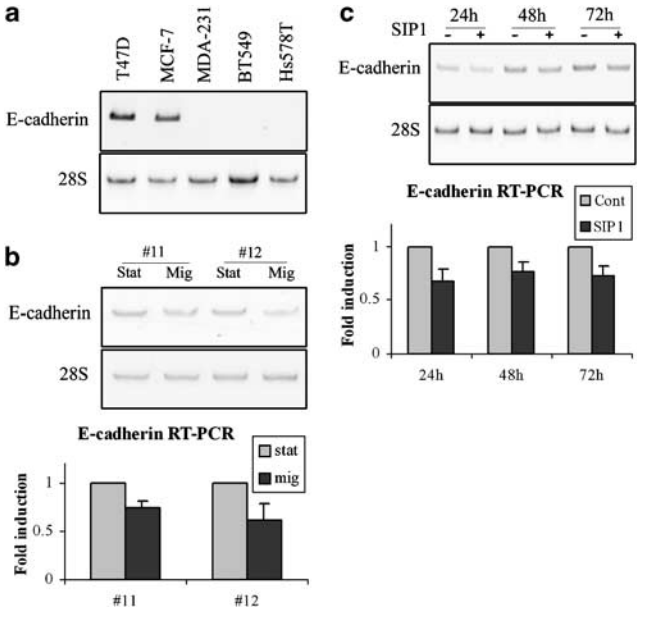

Figure 6 SIP1 expression inversely correlates with E-cadherin expression. RT–PCR analyses of E-cadherin in five breast tumor cell lines (**a**), in the migratory (mig) versus stationary (stat) subpopulations of VP-EGFP MCF10A cells plated in the migration assay (**b**) and in MCF10A cells transiently transfected with SIP1 cDNA for 24, 48 or 72 h (**c**). Quantifications of RT–PCR analyses of E-cadherin normalized for the 28S rRNA values in three independent experiments are shown for (**b**) and (**c**). Data are expressed as fold induction in the migratory subpopulation relative to the stationary subpopulation for (**b**) ($P<0.05$) and in the SIP1 transfectants relative to the backbone vector transfectants for (**c**) ($P<0.05$).

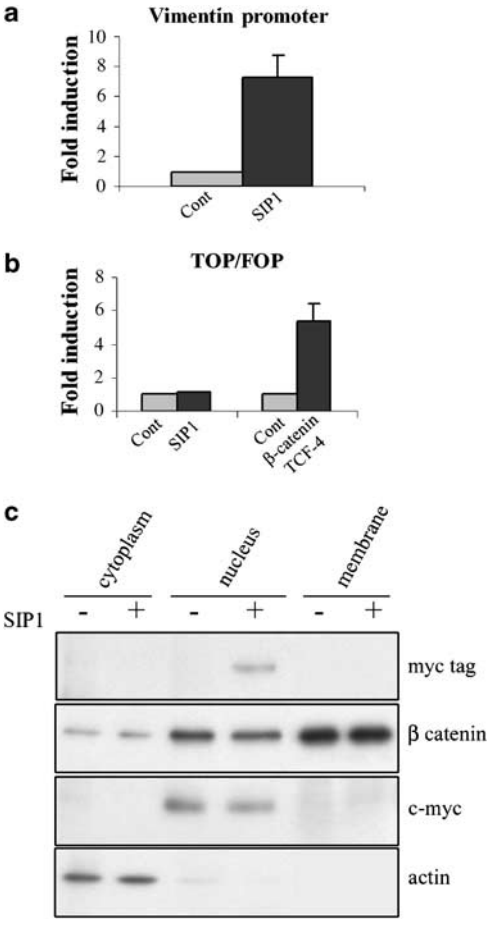

Figure 7 No implication of the β-catenin/TCF pathway in the regulation of vimentin by SIP1. (**a**) Vimentin promoter reporter assay. The human vimentin promoter luciferase reporter plasmid was cotransfected in MCF10A cells either with the SIP1 cDNA expression vector (SIP1) or with the corresponding control vector (Cont). Data are expressed as fold induction in SIP1 transfectants relative to the values obtained in the cells transfected with the backbone control vector ($P<0.01$). (**b**) TOP-FLASH/FOP-FLASH reporter assay. The TOP-FLASH or FOP-FLASH reporter plasmid was cotransfected in MCF10A cells with a control vector (Cont) or the SIP1 expression vector (SIP1). The normalized FOP values were subtracted from the normalized TOP values. Data are expressed as fold induction relative to the values obtained in the cells transfected with the control vector ($P>0.05$). Cotransfection with the β-catenin and TCF-4 expression vectors was performed as a control ($P<0.02$). (**c**) Western blotting analyses of β-catenin in cytosolic, nuclear and membranous fractions of MCF10A cells transfected either with the SIP1 expression vector (SIP1) or with the backbone control vector (Cont). The presence of the myc-tagged SIP1 is also shown in the nucleus of SIP1-transfected cells. Endogenous actin and c-myc expression were analysed as controls. A representative experiment is shown out of three independent experiments performed.

dynamic model allowed to clearly show the induction of vimentin during cell migration, discriminating a subpopulation of migratory, vimentin-positive cells from a vimentin-negative, stationary subpopulation within the same cell line (Gilles *et al*., 1999). Here, we were able to demonstrate increased SIP1 expression specifically in the vimentin-positive migratory subpopulation. In agreement with previous studies (Sommers *et al*., 1994; Comijn *et al*., 2001; Gilles *et al*., 2003), a lower level of E-cadherin was observed both in the invasive cell lines, as well as in the migratory subpopulation of MCF10A, also attesting the EMT-derived phenotype of these invasive and migratory cells expressing SIP1. In line with our observations, SIP1 expression has been associated with migratory and invasive mechanisms occurring during embryonic development. Indeed, a high level of SIP1 has been detected during the formation of the neural tube and this has been shown to play a key role in the migration of neural crest cells (Eisaki *et al*., 2000; van Grunsven *et al*., 2000; Van de Putte *et al*., 2003), a system largely described as a physiological archetypal model of EMT (Duband *et al*., 1995; Tucker, 2004). Also, an increased expression of SIP1 has been described in NMuMG cells which have undergone a TGFβ1-induced EMT characterized by decreased E-cadherin expression and increased N-cadherin expression (Maeda *et al*., 2005). Our results thus demonstrate a relationship between SIP1 and an EMT-derived phenotype characterized by vimentin expression, and further emphasize the implication of this relationship in dynamic cell migration.

We further observed that transfection of SIP1 cDNA in MCF10A cells increased vimentin expression both at the mRNA and protein level, which was associated with increased migratory ability. Inversely, the expression of

SIP1-specific shRNAs in MCF10A cells clearly diminished vimentin expression as well as their migratory properties. Strengthening these data, a diminution of vimentin expression following SIP1 siRNA transfection was also shown in BT549 breast tumor cells. Up to now, the implication of SIP1 in EMT phenomena associated with tumor cell invasion has been more particularly linked to its ability to repress E-cadherin, as shown in MDCK cells and in hepatocellular and colon epidermoid carcinoma cells transfected with SIP1 (Comijn *et al*., 2001; Miyoshi *et al*., 2004; Vandewalle *et al*., 2005). A repression of E-cadherin by SIP1 was accordingly observed in our cell systems. Overall, an increasing number of zinc-finger transcription factors, including Snail and Slug, both belonging to the Snail family, have been described as E-cadherin repressors and have been implicated in the regulation of EMT phenomena (Nieto, 2002; Come *et al*., 2004). Forcing the expression of these factors in a variety of epithelial cell systems was found to induce EMT processes characterized by decreased E-cadherin levels and by increased migratory/invasive properties (Cano *et al*., 2000; Hajra *et al*., 2002; Nieto, 2002; Come *et al*., 2004; Peinado *et al*., 2004). Accumulating data now also show that these factors can modulate the expression of other genes implicated in tumor cell invasion. For instance, they have been shown to downregulate other cell–cell contact molecules but also to upregulate 'mesenchymal' genes including fibronectin, vimentin and members of the matrix metalloproteases (MMP) family (Savagner *et al*., 1997; Cano *et al*., 2000; Hajra *et al*., 2002; Bolos *et al*., 2003; Ikenouchi *et al*., 2003; Yokoyama *et al*., 2003; Ohkubo and Ozawa, 2004; Vandewalle *et al*., 2005). Much less is known regarding the δEF1/ZEB family. Recent studies have nevertheless shown that SIP1-induced EMT in hepatocellular and in colon epidermoid carcinoma cells is also associated with an increased expression of N-cadherin and mesenchymal p120ctn isoforms (Vandewalle *et al*., 2005) as well as several members of the MMP family (Miyoshi *et al*., 2004). Thus, together with our observations that expression of endogenous vimentin and SIP1 associates with migratory/invasive abilities, these results suggest that SIP1 can contribute to the upregulation of vimentin transcription such as that occurs during epithelial cell migration/invasion.

The mechanism by which SIP1 regulates vimentin remains unclear. SIP1 has been described as a transcriptional repressor downregulating target genes through direct binding of bipartite elements made of one 5′-CACCT-3′ and one 5′-CACCTG-3′ sequence (Remacle *et al*., 1999). The fact that vimentin is upregulated by SIP1 and that no such bipartite element could be found in the vimentin promoter sequence suggested that vimentin regulation by SIP1 is most likely indirect. Considering the repressive effect of SIP1 effect on E-cadherin (Comijn *et al*., 2001; van Grunsven *et al*., 2003), it was tempting to speculate that SIP1 induction of vimentin could depend on the activation of the β-catenin/TCF pathway. Although it is not always observed (Comijn *et al*., 2001), diminished E-cadherin expression could indeed favor translocation of β-catenin in the nucleus where it can trigger the transcription of several target genes through binding with members of the TCF/LEF transcription factor family (Hecht and Kemler, 2000; Giles *et al*., 2003). Furthermore, vimentin has been shown to be a target of the β-catenin/TCF pathway (Gilles *et al*., 2003). However, our present results rather suggest that the β-catenin/TCF pathway is not activated following SIP1 transfection, as also observed by Comijn *et al*. (2001) in MDCK cells. Indeed, transfection of SIP1 cDNA into MCF10A cells did not lead to an increase in the TOP-FLASH reporter system though it activated the vimentin promoter. Also, in agreement with our TOP-FLASH results, we did not observe any accumulation of nuclear β-catenin in SIP1-transfected MCF10A cells. It has also to be noticed that SIP1 downregulation by siRNA in invasive BT549 cells, which do not express E-cadherin, can also modulate vimentin expression. Taken together, these data therefore suggest that regulation of vimentin by SIP1 can be independent of E-cadherin expression and does not necessarily rely in modulations of the β-catenin/TCF pathway. Nevertheless, many other indirect mechanisms could be involved. Additionally, the possibility that SIP1 could directly bind to and activate the vimentin promoter (through the binding of a single CACCT motif or another motif similar in sequence) cannot be excluded and is currently under investigation.

In conclusion, our results clearly demonstrate that SIP1 and vimentin expression correlate with a migratory/invasive phenotype and that SIP1 can regulate vimentin expression in epithelial breast tumor cells. Because of the established functional role of vimentin in cell migration, the upregulation of vimentin by SIP1 has implications for all processes requiring epithelial cell migration including tumor cell invasion.

Materials and methods

Cell culture

All human mammary epithelial cells used were obtained from the American Type Culture Collection (Rockville, MD, USA). MCF10A-VP-EGFP cells were generated previously by stable transfection of MCF10A cells with the VP-EGFP plasmid in which the human vimentin promoter controls the expression of EGFP (Gilles *et al*., 1999). MCF-7, T47D, MDA-MB-231, BT549 and Hs578T cells were cultured in Dulbecco's modified Eagle's medium (DMEM) containing 10% FCS. MCF10A cells were grown in a 1:3 (v/v) mixture of HAM F12 and DMEM, supplemented with 20 μg/ml of adenine, 5 μg/ml of insulin, 0.5 μg/ml of hydrocortisone, 2 ng/ml of EGF, 5 μg/ml of transferrin, 1.5 ng/ml of triiodothyronin and 10% FCS.

Primary epithelial cells and primary fibroblasts were isolated from human polyps as previously described (Million *et al*., 2001). Primary epithelial cells were allowed to differentiate, as attested by the presence of ciliated cells, in a transwell chamber coated with collagen type I for 12 days (Million *et al*., 2001).

In vitro *migration assay*

In order to sort by FACS the vimentin-expressing migratory cells from the stationary, vimentin-negative cells, we used two clones of MCF10A-VP-EGFP expressing the EGFP reporter

gene driven by the vimentin promoter (MCF10A-VP-EGFP #11 and #12 as also described in Gilles *et al*., 1999). These cells were analysed in a migration assay as described previously (Gilles *et al*., 1999). Briefly, 5×10^4 cells were seeded in growth medium inside a 6-mm glass ring. At 24 h after plating, the glass ring was removed and the cells were covered either with complete growth medium (containing FCS and EGF) or with FCS-free growth medium in order to examine the implication of EGF. In this model, the cells migrate as an outgrowth from the confluent area initially delimited by the ring. We have previously shown that cells at the periphery of the outgrowth are implicated in an oriented migration and express vimentin and GFP. In contrast, the cells in the area initially delimited by the ring are rather stationary and do not express vimentin nor GFP (Gilles *et al*., 1999). At 48 h after the removal of the ring, the cells were collected by trypsinization of 24 migration assays and were sorted by FACS (FACSVantage-SE, Becton Dickinson, Erembodegem, Belgium) into EGFP-positive and EGFP-negative populations, which were then used for RNA extraction and RT–PCR analysis.

Immunofluorescence
Cells cultured in the migration assay on glass coverslips were fixed in paraformaldehyde (4% in PBS) for 10 min and then permeabilized with 0.1% Triton X-100 for 1 min at room temperature. The coverslips were then blocked for 30 min with 3% BSA in PBS. After several washes with PBS, fixed monolayers were incubated for 1 h with a monoclonal antibody to vimentin (clone V9, Dako, Glostrup, Denmark) and then exposed to a TRITC-conjugated rabbit anti-mouse antibody (Dako). Finally, nuclei were labeled with 4′,6-diamidino-2-phenylindole (DAPI; 1 μg/ml) for 20 min. The coverslips were then mounted with Aquapolymount antifading solution (Agar, UK) onto glass slides and observed under a fluorescence microscope (Olympus, Tokyo, Japan).

Plasmids
The vimentin promoter luciferase reporter vector (VimPro) used in this study has been characterized previously (Gilles *et al*., 2003). This plasmid consists of the human vimentin promoter cloned into the firefly luciferase reporter plasmid pGL-3 (Promega, Madison, WI, USA).

The expression vector for the SIP1 cDNA encoding a myc-tagged protein has been described previously (Verschueren *et al*., 1999; Comijn *et al*., 2001).

An expression vector encoding a mutated form of β-catenin which is less susceptible to degradation was kindly provided by Dr K Orford and Dr S Byers (Lombardi Cancer Center, Georgetown University, Washington, DC, USA) (Orford *et al*., 1997). Dr HC Clevers (University Hospital, Utrecht, The Netherlands) donated the expression vector encoding human TCF-4 (pCDNA-hTCF4) and the TOP-FLASH and FOP-FLASH plasmids containing, respectively, three wild-type (5′-CCTTTGATC-3′: TOP-FLASH) or mutated (5′-CCTTTGGCC-3′: FOP-FLASH) copies of the β-catenin/TCF-binding sites upstream of a minimal c-*fos* promoter driving the expression of firefly luciferase (Korinek *et al*., 1997; van de Wetering *et al*., 1997).

Luciferase reporter assay
Transient transfections were performed with Fugene transfection reagent (Roche, Branchburg, NJ, USA) on 50 000 cells plated in a 24-well plate half an hour before the addition of the DNA/Fugene mixture.

For the determination of the vimentin promoter induction by SIP1, each well was supplemented with a mixture containing 20 μl of serum-free DMEM, 0.6 μl of Fugene and 0.2 μg of the promoter reporter construct (either VimPro, TOP-FLASH or FOP-FLASH reporter construct), 0.2 μg of the SIP1 expression vector (or the backbone vector control) and 1.6 ng of the Renilla luciferase reporter phRG-TK (Promega) used as an internal control. For β-catenin/TCF-4 induction, each well was incubated with a mixture containing 20 μl of serum-free DMEM, 0.6 μl of Fugene, 0.15 μg of the firefly luciferase reporter plasmid (either VimPro, TOP-FLASH or FOP-FLASH reporter construct), 0.15 μg of the β-catenin expression vector (or the corresponding backbone vector), 0.15 μg of the TCF-4 expression vector (or the corresponding backbone vector) and 1.6 ng of the Renilla luciferase vector phRG-TK.

At 24 h after transfection, the cells were lysed in 100 μl of lysis buffer followed by determination of luciferase activity in 20 μl of lysate with a luminometer using the Dual Luciferase Assay System (Promega). The firefly luciferase activity was normalized to the activity of the Renilla luciferase used as internal control. Results were expressed as fold induction, calculated by dividing the normalized values obtained following cDNA transfection by the normalized values obtained following transfection of the corresponding backbone expression vector. To assess the β-catenin/TCF/LEF activities using the TOP/FOP-FLASH reporter system, the normalized values obtained with the FOP-FLASH reporter plasmid were subtracted from the normalized values obtained with the TOP-FLASH reporter plasmid. Results were then expressed as fold induction relative to the value obtained in the cells transfected with the control vector. Each experiment was performed at least three times in triplicate. Data are expressed as means $\pm$ s.e. A one-sample *t*-test was performed and a *P*-value < 0.05 was considered significant.

Transient transfections of Smad interacting protein-1 cDNA
To study the regulation of the endogenous vimentin gene by SIP1, 150 000 MCF10A cells plated in six-well plates were transiently transfected with the SIP1 expression vector using Lipofectamine 2000 transfection reagent (Invitrogen, Carlsbad, CA, USA). At 24 h after plating, transfection was carried out as recommended by the manufacturer by adding, in each well, a mixture containing 500 μl of serum-free medium, 3 μl of Lipofectamine 2000 and 2 μg of the SIP1 expression vector. As control, cells were transfected with the corresponding backbone vector. At 24, 48 and 72 h after transfection, cells were collected for RT–PCR or Western blotting analyses. A control transfection condition using a plasmid encoding GFP (pEGFP-IRESpuro, Clontech, CA, USA) was always performed in parallel to determine the transfection efficiency. All experiments were set up to obtain at least 70% of transfected cells.

Transfection of small interfering RNA
Two 19-nt-specific sequences were selected in the coding sequence of SIP1 to generate 21-nt sense and 21-nt antisense strands of the type (19N) TT (N, any nucleotide). The sense and antisense strands were then annealed to obtain duplexes with identical 3′ overhangs. The sequences were submitted to a BLAST search against the human genome to ensure the specificity of the small interfering RNA (siRNA) to the targeted sequence. Two duplexes, which do not recognize any sequence in the human genome, were used as controls. The 19-nt-specific sequences for the two SIP1 siRNAs are as follows: SIP1 Si1, 5′-GGUAAUCGCAAGUUCAAAU-3′; SIP1 Si2, 5′-GAACAGACAGGCUUACUUA-3′. For transfection of the siRNA duplexes, 75 000 cells were plated in six-well plates in 2 ml/well of culture medium. At 24 h after plating,

the cells were transfected by phosphate calcium precipitation by adding in each well 200 μl of a mixture containing the siRNA duplexes (20 nM), 140 mM NaCl, 0.75 mM Na_2HPO_4, 6 mM glucose, 5 mM KCl, 25 mM HEPES and 125 mM $CaCl_2$. At 24 h after transfection, the cells were extensively washed with PBS and incubated for 48 h in culture medium before they were harvested for RT–PCR analyses or Western blotting analyses. The transfection of an FITC-labelled control siRNA (Eurogentec, Belgium) was also performed in parallel and revealed an uptake of the siRNA in 100% of the cells.

Transduction of the lentiviral vector for SIP1 short hairpin RNA
A SIP1-specific siRNA sequence was designed using selection criteria as described (Brummelkamp *et al*., 2002; Ui-Tei *et al*., 2004). A double PCR approach was used to create shRNA expression cassettes containing the H1 promoter and both the sense and antisense shRNA sequences with a loop sequence in between. In a first step, PCR was performed using pSuper plasmid (Brummelkamp *et al*., 2002) as a template, the H1 promoter primer 5′-CTGCAGGAATTCGAACGCTGACGT CATCAA-3′ and the sense shRNA oligonucleotide 5-AAATC TCTTGAATTTAACAATACCCAGCTCCGGGGATCTGT GGTCTCATACAGAACTTATAA-3′ (SEC1 = SIP1sh1) or 5′- TGTTCTCTTGAAACAAAGGTAACGTTCATGCGGG GATCTGTGGTCTCATACAGAACTTATAA-3′ (SEC8 = SIP1sh2). This PCR product was a template for a second PCR reaction with the same H1 promoter primer and the antisense shRNA oligonucleotide 5′-CCATCGATAAGCTTT TTTTCCAAAAAAGGAGCTGGGTATTGTTAAATCTCT TGAATTTA-3′ (SEC1 = SIP1sh1) or 5′-CCATCGATAAGC TTTTTTTCCAAAAAAGCATGAACGTTACCTTTGTTC TCTTGAAACAA-3′ (SEC8 = SIP1sh2). The shRNA expression cassette was cloned in the lentiviral pLV-TH vector (Wiznerowicz and Trono, 2003) using *Eco*RI and *Cla*I restriction sites.

For lentivirus production, 1.2 million cells of the packaging cell line HEK293T were seeded in a 25-cm^2 flask. After 24 h, 3 μg of the pLV-THshRNA construct or empty vector, 3 μg of the packaging plasmid pCMVdR8.91 and 1.5 μg of the envelope plasmid pMD2G-VSVG were first precipitated together and then transfected into the HEK293T cells using the calcium phosphate precipitation method. The DNA was premixed with 50 μl of 2 M $CaCl_2$ and 190 μl TE buffer and then slowly added to 250 μl 2 × HBS. The mixture was put on a shaker for 15 min before it was added to the cells. After 8 h, the cells were washed and incubated for 48 h in 4 ml fresh culture medium. The virus-containing medium was then harvested and filtered through a 0.45 μm low protein binding filter unit (Millipore, Billerica, MA, USA). Aliquots were stored at −70°C.

Transduction of the MCF10A cells was performed by mixing 50 000 cells with 200 μl viral supernatant in a 96-well plate and three replicates of each transduction were made. These mixtures were centrifuged for 1.5 h at 32°C and 1500 r.p.m. before putting them in the 37°C incubator. After 24 h, the cells were trypsinized and replicates were pooled in a 24-well plate together with 800 μl fresh viral supernatant. The mixtures were again centrifuged as mentioned above and incubated for 24 h before replacing the medium with fresh culture medium.

Transduction efficiencies were determined by measuring EGFP expression using FACS analysis (Epics Altra from Beckman Coulter, Fullerton, CA, USA). Subsequently, the cells were sorted to obtain cell populations with more than 90% EGFP-positive cells.

Western blotting analyses
Total protein extracts were prepared in RIPA buffer (50 mM Tris, pH 7.4, 150 mM NaCl, 1% (v/v) Igepal, 1% (w/v) sodium deoxycholate, 5 mM iodoacetamide, 0.1% (w/v) SDS), containing complete protease inhibitor cocktail (Roche). To examine the subcellular distribution of β-catenin, cytosolic, membranous and nuclear extracts of MCF10A cells transfected with the SIP1 expression vector (or the corresponding backbone vector) for 48 h were prepared using the ProteoExtract Subcellular Proteome Extraction Kit (Calbiochem, LaJolla, CA, USA). Protein concentration was determined with the DC protein assay (BioRad, Richmond, CA, USA). In all, 10 μg or 500 ng of total protein were separated on 15% SDS–PAGE gels for analysis of vimentin in MCF10A and BT549 cells, respectively. Total protein extract of MCF10A cells (500 ng) was separated on 10% SDS–PAGE gels for E-cadherin analysis. In total, 4 μg of cytosolic or nuclear extracts and 1 μg of membranous extracts of MCF10A cells were separated on 10% SDS–PAGE to analyse the expression of β-catenin. Proteins were transferred to PVDF membranes (NEN, Boston, MA, USA), which were then blocked with 5% milk (w/v) + 0.1% Tween 20 (w/v) in PBS for 2 h. They were then exposed to primary antibodies overnight at 4°C: a monoclonal antibody (mAb) to vimentin (clone V9, Dako), an mAb to E-cadherin (BD Transduction Laboratories, San Jose, CA) or an mAb to β-catenin (either from BD Transduction Laboratories or clone 8E4 from AG Scientific, CA, USA, which is a specific antibody for the unphosphorylated form of β-catenin). The filters were then incubated with a horseradish peroxidase-conjugated swine anti-mouse antibody (Dako). Signals were detected with an enhanced chemiluminescence (ECL +) kit (Amersham Pharmacia Biotech, Buckinghamshire, UK). Subsequent detection of actin (using a rabbit antibody to actin, clone A2066, Sigma-Aldrich, St Louis, MO, USA), or c-myc (using an mAb to c-myc, clone 9E10, Sigma) was performed on the same filters as a control. Western blotting analyses were performed on three independent experiments and a representative experiment is shown in the figures.

RT–PCR analysis
Total RNA was extracted with an RNA isolation kit (Roche). RT–PCR was performed using 10 ng of total RNA and the GeneAmp Thermostable RNA PCR Kit (Perkin Elmer, Foster City, CA, USA). Forward and reverse primers (Eurogentec, Seraing, Belgium) were as follows: vimentin primers (forward 5′-GACAATGCGTCTCTGGCACGTCTT-3′, reverse 5′-TCCTCCGCCTCCTGCAGGTTCTT-3′), SIP1 primers (forward 5′-AGTCCATGCGAACTGCCATCTGAT-3′, reverse 5′- CTGGACCATCTACAGAGGCTTGTA-3′), E-cadherin primers: (forward 5′-CCCATCAGCTGCCCAGAAAATGA A-3′, reverse 5′- CTGTCACCTTCAGCCATCCTGTTT-3′), 28S rRNA primers (forward 5′-GTTCACCCACTAATAGGG AACGTGA-3′, reverse 5′-GGATTCTGACTTAGAGGCGT TCAGT-3′). Reverse transcription was performed at 70°C for 15 min. Products were separated on acrylamide gels, stained with SYBR Gold (Molecular Probes, Eugene, OR, USA) and quantified by fluorimetric scanning (LAS-1000, Fuji, Stamford, CT, USA). Quantification was performed by normalization of the values obtained for 28S rRNA amplification. For SIP1 cDNA transfection or RNAi experiments, results were expressed as fold induction calculated by dividing the normalized value of a given condition (SIP1 cDNA transfection, SIP1 siRNA transfection or SIP1 shRNA transduction) by the normalized value of the corresponding control. Each experiment was performed at least three times. Data are

expressed as means ± s.e. A one-sample *t*-test was performed and a *P*-value <0.05 was considered significant.

Boyden chamber invasion assay

The migratory properties of MCF10A cells transfected with SIP1 cDNA for 48 h or transduced with the SIP1shRNA lentiviral vector were assessed using the Boyden chamber assay. Cells (100 000) were suspended in 300 μl of serum-free medium supplemented with 0.1% BSA and placed in the upper compartment of a 24-well transwell (Costar, NY, USA). The lower compartment was filled with 600 μl of medium containing 10% FCS and 1% BSA. After 6 h of incubation at 37°C, the filters were fixed in methanol for 10 min and stained with Giemsa for 30 min. Cells on the upper surface of the filters were wiped away with a cotton swab. Migration was quantified by counting the number of cells on the lower surface of the filters. Experiments were performed at least three times in triplicate. Data are expressed as means ± s.e. A one-sample *t*-test was performed and a *P*-value <0.05 was considered significant.

Acknowledgements

We thank Dr H Clevers for the TOP-FLASH, the FOP-FLASH and TCF-4 expression vector and Dr K Orford and Dr S Byers for the β-catenin expression vector. This work was supported by grants from the 'Communauté française de Belgique (Actions de Recherches Concertées)', the Commission of European Communities (European Union Framework Programs 5 and 6, BRECOSM), the 'Fonds de la Recherche Scientifique Médicale', the 'Fonds National de la Recherche Scientifique' (FNRS, Belgium), the 'Fédération Belge Contre le Cancer', the 'coopération C.G.R.I.-F.N.R.S.-INSERM', the 'Fonds spéciaux de la Recherche (University of Liège), the 'Centre Anticancéreux près l'Université de Liège', the Fortis Banque Assurances, the 'Fondation Léon Fredericq' (University of Liège), the D.G.T.R.E. from the 'Région Wallonne', the 'Fonds d'Investissements de la Recherche Scientifique (CHU, Liège, Belgium)', the Interuniversity Attraction Poles Program – Belgian Science Policy (Brussels, Belgium). CG is a Research Associate from the FNRS (Belgium), SB is an FRIA grant holder from the F.N.R.S., MM is a Research Fellow from the F.N.R.S, and GB is a postdoctoral researcher with the FWO (Belgium).

References

Bienz M. (2005). *Curr Biol* **15**: R64–R67.
Bolos V, Peinado H, Perez-Moreno MA, Fraga MF, Esteller M, Cano A. (2003). *J Cell Sci* **116**: 499–511.
Brummelkamp TR, Bernards R, Agami R. (2002). *Science* **296**: 550–553.
Cano A, Perez-Moreno MA, Rodrigo I, Locascio A, Blanco MJ, del Barrio MG *et al*. (2000). *Nat Cell Biol* **2**: 76–83.
Come C, Arnoux V, Bibeau F, Savagner P. (2004). *J Mammary Gland Biol Neoplasia* **9**: 183–193.
Comijn J, Berx G, Vermassen P, Verschueren K, van Grunsven L, Bruyneel E *et al*. (2001). *Mol Cell* **7**: 1267–1278.
Duband JL, Monier F, Delannet M, Newgreen D. (1995). *Acta Anat (Basel)* **154**: 63–78.
Eckes B, Colucci-Guyon E, Smola H, Nodder S, Babinet C, Krieg T *et al*. (2000). *J Cell Sci* **113**: 2455–2462.
Eckes B, Dogic D, Colucci-Guyon E, Wang N, Maniotis A, Ingber D *et al*. (1998). *J Cell Sci* **111**: 1897–1907.
Eisaki A, Kuroda H, Fukui A, Asashima M. (2000). *Biochem Biophys Res Commun* **271**: 151–157.
Giles RH, van Es JH, Clevers H. (2003). *Biochim Biophys Acta* **1653**: 1–24.
Gilles C, Newgreen D, Sato H, Thompson EW. (2004). *Rise and Fall of Epithelial Phenotype* In: Savagner P (ed). Eurekah.com and Kluwer Academic/Plenum Publishers: New York, (Chapter 2).
Gilles C, Polette M, Mestdagt M, Nawrocki-Raby B, Ruggeri P, Birembaut P *et al*. (2003). *Cancer Res* **63**: 2658–2664.
Gilles C, Polette M, Zahm JM, Tournier JM, Volders L, Foidart JM *et al*. (1999). *J Cell Sci* **112**: 4615–4625.
Gilles C, Thompson EW. (1996). *Breast J* **2**: 83–96.
Goldman RD, Chou YH, Prahlad V, Yoon M. (1999). *FASEB J* **13**(Suppl 2): S261–S265.
Gonzales M, Weksler B, Tsuruta D, Goldman RD, Yoon KJ, Hopkinson SB *et al*. (2001). *Mol Biol Cell* **12**: 85–100.
Gotzmann J, Mikula M, Eger A, Schulte-Hermann R, Foisner R, Beug H *et al*. (2004). *Mutat Res* **566**: 9–20.
Guarino M. (1995). *Histol Histopathol* **10**: 171–184.
Hajra KM, Chen DYS, Fearon ER. (2002). *Cancer Res* **62**: 1613–1618.
Hecht A, Kemler R. (2000). *EMBO Rep* **1**: 24–28.
Helfand BT, Chang L, Goldman RD. (2004). *J Cell Sci* **117**: 133–141.
Hendrix MJ, Seftor EA, Chu YW, Trevor KT, Seftor RE. (1996). *Cancer Metast Rev* **15**: 507–525.
Hendrix MJ, Seftor EA, Seftor RE, Trevor KT. (1997). *Am J Pathol* **150**: 483–495.
Homan SM, Mercurio AM, LaFlamme SE. (1998). *J Cell Sci* **111**: 2717–2728.
Ikenouchi J, Matsuda M, Furuse M, Tsukita S. (2003). *J Cell Sci* **116**: 1959–1967.
Korinek V, Barker N, Morin PJ, van Wichen D, de Weger R, Kinzler KW *et al*. (1997). *Science* **275**: 1784–1787.
Kreis S, Schonfeld HJ, Melchior C, Steiner B, Kieffer N. (2005). *Exp Cell Res* **305**: 110–121.
Maeda M, Johnson KR, Wheelock MJ. (2005). *J Cell Sci* **118**: 873–887.
Maniotis AJ, Chen CS, Ingber DE. (1997). *Proc Natl Acad Sci USA* **94**: 849–854.
Million K, Tournier F, Houcine O, Ancian P, Reichert U, Marano F. (2001). *Am J Resp Cell Mol Biol* **25**: 744–750.
Miyoshi A, Kitajima Y, Sumi K, Sato K, Hagiwara A, Koga Y *et al*. (2004). *Br J Cancer* **90**: 1265–1273.
Nawrocki RB, Polette M, Gilles C, Clavel C, Strumane K, Matos M *et al*. (2001). *Int J Cancer* **93**: 644–652.
Nieto MA. (2002). *Nat Rev Mol Cell Biol* **3**: 155–166.
Ohkubo T, Ozawa M. (2004). *J Cell Sci* **117**: 1675–1685.
Orford K, Crockett C, Jensen JP, Weissman AM, Byers SW. (1997). *J Biol Chem* **272**: 24735–24738.
Peinado H, Portillo F, Cano A. (2004). *Int J Dev Biol* **48**: 365–375.
Ramaekers FC, Haag D, Kant A, Moesker O, Jap PH, Vooijs GP. (1983). *Proc Natl Acad Sci USA* **80**: 2618–2622.
Remacle JE, Kraft H, Lerchner W, Wuytens G, Collart C, Verschueren K *et al*. (1999). *EMBO J* **18**: 5073–5084.
Savagner P. (2001). *BioEssays* **23**: 912–923.
Savagner P, Yamada KM, Thiery JP. (1997). *J Cell Biol* **137**: 1403–1419.
Singh S, Sadacharan S, Su S, Belldegrun A, Persad S, Singh G. (2003). *Cancer Res* **63**: 2306–2311.
Sommers CL, Byers SW, Thompson EW, Torri JA, Gelmann EP. (1994). *Breast Cancer Res Treat* **31**: 325–335.

Staal FJ, Noort MM, Strous GJ, Clevers HC. (2002). *EMBO Rep* **3**: 63–68.
Steinert PM, Roop DR. (1988). *Annu Rev Biochem* **57**: 593–625.
Svitkina TM, Verkhovsky AB, Borisy GG. (1996). *J Cell Biol* **135**: 991–1007.
Thiery JP. (2002). *Nat Rev Cancer* **2**: 442–454.
Thompson EW, Paik S, Brunner N, Sommers CL, Zugmaier G, Clarke R *et al*. (1992). *J Cell Physiol* **150**: 534–544.
Tsuruta D, Jones JC. (2003). *J Cell Sci* **116**: 4977–4984.
Tucker RP. (2004). *Int J Biochem Cell Biol* **36**: 173–177.
Ui-Tei K, Naito Y, Takahashi F, Haraguchi T, Ohki-Hamazaki H, Juni A *et al*. (2004). *Nucleic Acids Res* **32**: 936–948.
Van Aken E, De Wever O, Correia da Rocha AS, Mareel M. (2001). *Virchows Arch* **439**: 725–751.
Van de Putte T, Maruhashi M, Francis A, Nelles L, Kondoh H, Huylebroeck D *et al*. (2003). *Am J Hum Genet* **72**: 465–470.
Vandewalle C, Comijn J, De Craene B, Vermassen P, Bruyneel E, Andersen H *et al*. (2005). *Nucleic Acids Res* **33**: 6566–6578.
van de Wetering M, Cavallo R, Dooijes D, van Beest M, van Es J, Loureiro J *et al*. (1997). *Cell* **88**: 789–799.
van Grunsven LA, Michiels C, Van de Putte T, Nelles L, Wuytens G, Verschueren K *et al*. (2003). *J Biol Chem* **278**: 26135–26145.
van Grunsven LA, Papin C, Avalosse B, Opdecamp K, Huylebroeck D, Smith JC *et al*. (2000). *Mech Dev* **94**: 189–193.
Verschueren K, Remacle JE, Collart C, Kraft H, Baker BS, Tylzanowski P *et al*. (1999). *J Biol Chem* **274**: 20489–20498.
Wiznerowicz M, Trono D. (2003). *J Virol* **77**: 8957–8961.
Wu AL, Wang J, Zheleznyak A, Brown EJ. (1999). *Mol Cell* **4**: 619–625.
Yokoyama K, Kamata N, Fujimoto R, Tsutsumi S, Tomonari M, Taki M *et al*. (2003). *Int J Oncol* **22**: 891–898.

Oncogene (2009), 1–11

www.nature.com/onc

ORIGINAL ARTICLE

Fhit regulates invasion of lung tumor cells

A Joannes[1,2], A Bonnomet[3], S Bindels[3], M Polette[1,2,4], C Gilles[3], H Burlet[1,2], J Cutrona[1,5], J-M Zahm[1,2], P Birembaut[1,2,4] and B Nawrocki-Raby[1,2]

[1]INSERM, U903, Reims, France; [2]Univ Reims Champagne Ardenne, IFR53, UMR-S903, Reims, France; [3]Univ Liège, CHU Sart-Tilman, Laboratoire de Biologie des Tumeurs et du Développement, Liège, Belgium; [4]CHU Reims, Hôpital Maison Blanche, Laboratoire Pol Bouin, Reims, France and [5]Univ Reims Champagne Ardenne, CRESTIC, Reims, France

In many types of cancers, the *fragile histidine triad* (*Fhit*) gene is frequently targeted by genomic alterations leading to a decrease or loss of gene and protein expression. *Fhit* has been described as a tumor suppressor gene because of its ability to induce apoptosis and to inhibit proliferation of tumor cells. Moreover, several studies have shown a correlation between the lack of Fhit expression and tumor aggressiveness, thus suggesting that Fhit could be involved in tumor progression. In this study, we explored the potential role of Fhit during tumor cell invasion. We first showed that a low Fhit expression is associated with *in vivo* and *in vitro* invasiveness of tumor cells. Then, we showed that Fhit overexpression in Fhit-negative highly invasive NCI-H1299 cells by transfection of Fhit cDNA and Fhit inhibition in Fhit-positive poorly invasive HBE4-E6/E7 cells by transfection of Fhit small interfering RNA induce, respectively, a decrease and an increase in migratory/invasive capacities. These changes in cell behavior were associated with a reorganization of tight and adherens junction molecules and a regulation of matrix metalloproteinase and vimentin expression. These results show that Fhit controls the invasive phenotype of lung tumor cells by regulating the expression of genes associated with epithelial–mesenchymal transition.
Oncogene advance online publication, 23 November 2009; doi:10.1038/onc.2009.418

Keywords: Fhit; tumor invasion; epithelial–mesenchymal transition; cell–cell adhesion molecules; matrix metalloproteinases; vimentin

Introduction

The *fragile histidine triad* (*Fhit*) gene located at chromosome region 3p14.2 encompassing the common fragile site FRA3B spans about 2 Mb of the human genome. *Fhit* encodes a 1.1 kb mRNA and a 16.8 kDa protein ubiquitously expressed in epithelial tissues (Ohta *et al*., 1996). Fhit behaves *in vitro* as a typical diadenosine triphosphate (Ap3A) hydrolase, but little is known about its physiological function (Barnes *et al*., 1996; Pekarsky *et al*., 2002). The lack or decrease of Fhit expression, which is a consequence of chromosomal aberrations such as deletions, loss of heterozygosity, promoter methylation or abnormal transcripts, is a common event in most human cancers (Ishii *et al*., 2001; Pekarsky *et al*., 2002; Huebner and Croce, 2003). Several studies have indeed shown that Fhit is inactivated in lung, breast, esophagus, stomach, kidney and cervix carcinomas (Negrini *et al*., 1996; Ohta *et al*., 1996; Sozzi *et al*., 1996; Ishii *et al*., 2001; Huebner and Croce, 2003). After its identification in 1996 (Ohta *et al*., 1996), *Fhit* has been rapidly proposed as a tumor suppressor gene (Siprashvili *et al*., 1997; Ishii *et al*., 2001). *Fhit* gene delivery in various cancer cells has been shown to suppress tumorigenicity *in vitro* and *in vivo* in nude mice, by inducing caspase-dependent apoptosis and inhibiting cell proliferation (Siprashvili *et al*., 1997; Ji *et al*., 1999; Dumon *et al*., 2001; Roz *et al*., 2002; Cavazzoni *et al*., 2004; Campiglio *et al*., 2006). The exact molecular pathway of the tumor suppressive function of Fhit is, however, still unclear. Interestingly, the enzymatic activity of Fhit is not required but the binding to its substrate Ap3A seems to be necessary (Siprashvili *et al*., 1997; Pace *et al*., 1998; Trapasso *et al*., 2003; Campiglio *et al*., 2006). Moreover, the reduced expression of Fhit has been correlated with poor differentiation, histological grade, positive node status, distant metastases and worse prognosis in different types of cancers such as tongue, gastric, colon, cervical, breast and lung carcinomas (Huebner and Croce, 2003; Nakata *et al*., 2006). These data showing that Fhit inactivation is associated with tumor aggressiveness thus suggest that Fhit could also have an involvement during tumor cell invasion.

The acquisition of invasive properties by tumor cells requires the loss of typical epithelial features (in particular, the decrease of cell cohesion and the loss of cell polarity) and the gain of mesenchymal characteristics (in particular, capacities to degrade the extracellular matrix (ECM) and to migrate), a phenomenon referred to as epithelial–mesenchymal transition (EMT) (Lee *et al*., 2006; Gavert and Ben Ze'ev, 2008). Among the mechanisms largely associated with this process is the disruption of intercellular adhesion, a consequence of the reorganization of E-cadherin/β-catenin complexes of adherens junctions (Van Aken *et al*., 2001; Lee *et al*., 2006). The loss of the E-cadherin-mediated cell adhesion

Correspondence: Dr B Nawrocki-Raby, INSERM, UMRS 903, CHU Maison Blanche, 45 rue Cognacq-Jay, F-51100 Reims, France.
E-mail: beatrice.raby@univ-reims.fr
Received 13 May 2009; revised 11 September 2009; accepted 18 October 2009

is correlated with cell invasion and the re-expression of E-cadherin in highly invasive tumor cells reduces their invasive potential (Van Aken *et al*., 2001). Besides its structural role in adherens junction assembly, E-cadherin is also able to sequester to the cell membrane several co-transcriptional factors that can themselves modulate the expression of invasion-associated genes. In particular, its cytoplasmic binding partner β-catenin, once released from cell–cell contacts, accumulates in the cytoplasm and can then translocate to the nucleus, where it forms a complex with T-cell factor (TCF)/lymphoid enhancer factor (LEF) family members (Gavert and Ben Ze'ev, 2007; Polette *et al*., 2007). Even though less documented, the disorganization of occludin/zonula occludens (ZO)-1 tight junction complexes has also been shown to be a hallmark of a migratory/invasive phenotype *in vivo* and *in vitro* (Tobioka *et al*., 2004; Polette *et al*., 2005, 2007; Lee *et al*., 2006). Furthermore, similar to β-catenin, ZO-1 can also shuttle between the plasma membrane and the cytosol or the nucleus and intervene in signaling events promoting tumor cell invasion (Reichert *et al*., 2000; Polette *et al*., 2005, 2007). Besides the loss of cell–cell contacts, tumor invasion is also characterized by the production of matrix metalloproteinases (MMPs) by tumor cells themselves (Polette *et al*., 2004; Lee *et al*., 2006). MMPs constitute a family of secreted and cell surface enzymes that are able to degrade almost all ECM components and that have been shown to be overexpressed in numerous cancers (Chang and Werb, 2001; Polette *et al*., 2004). Because of their selective ability to degrade type-IV collagen, which is a major component of the basement membrane, MMP-2 and -9 have been shown to be involved in tumor invasion *in vitro* and *in vivo* (Polette *et al*., 2004). Membrane-type 1-MMP (MT1-MMP) also has a major involvement in the tumor invasion process not only through its degradative activities against structural ECM components, cell adhesion molecules and some cytokines but also through its function as the physiological activator of MMP-2 (Seiki, 2003). Moreover, the *de novo* expression of vimentin by tumor epithelial cells is an event also frequently linked to EMT-associated tumor cell invasion (Gilles and Thompson, 1996; Gilles *et al*., 1996). Vimentin is a type III intermediate filament protein expressed in cells of mesenchymal origin in adult differentiated tissues. Vimentin has also been associated with and is functionally implicated in epithelial cell migration and invasion (Hendrix *et al*., 1997; Gilles *et al*., 1999). Finally, several signaling pathways, such as transforming growth factor-β, nuclear factor-κB, Wnt and RTKs, have been described as EMT inducers because of their ability to activate transcription factors of the Snail, Twist and ZEB1 families (Gavert and Ben Ze'ev, 2008).

In this study, we investigated the potential role of *Fhit* during tumor cell invasion and particularly its capacities to regulate the invasive phenotype of tumor cells. Accordingly, we analysed the consequences of Fhit expression modulation in two lung cancer cell lines with different invasive capacities. We observed that Fhit controls cell migration and invasion by regulating EMT key events such as cell–cell adhesion and MMP (MMP-2, MMP-9, MT1-MMP) and vimentin expression.

Results

Loss of Fhit expression is associated with tumor invasion in vivo *and* in vitro

Expression of *Fhit* mRNA was detected by RT–PCR analysis in a series of non-small cell lung cancer (NSCLC). We found that *Fhit* was expressed significantly less in lung carcinomas (median: 1.30, min–max: 0.00–3.10) than in normal tissues (median: 3.05, min–max: 0.86–9.80) ($P<0.001$) (Figure 1a). In squamous-cell carcinomas, we also observed that Fhit expression was significantly reduced in tumors with lymph node involvement (N1 and N2 status) (median: 1.24, min–max: 0.33–2.56) compared to tumors without lymph node involvement (N0 status) (median: 2.20, min–max: 1.30–3.10) ($P<0.05$) (Figure 1b). According to the tumor–node–metastasis (TNM) classification, the *Fhit* mRNA level was also lower in stage II/III squamous-cell carcinomas (median: 1.27, min–max: 0.33–2.56) than in stage I tumors (median: 2.25, min–max: 1.54–3.10) ($P<0.05$) (Figure 1c). In addition, patients with a high level of *Fhit* mRNA tended to survive longer than patients with a weak level (data not shown). Furthermore, in squamous-cell carcinomas, absence of Fhit expression in tumor clusters was consistently observed at the invading front and in tumor cells infiltrating the stroma as shown by immunohistochemistry (Figure 1d).

To examine the relationship between Fhit expression and *in vitro* invasive capacities, we compared the level of Fhit analysed by western blotting (Figure 2a) in various lung and breast carcinoma cell lines checked for their invasive capacities in a modified Boyden chamber assay (Figure 2b). We found that Fhit was not expressed by the most invasive cell lines (Hs578T, BEAS-2B, BZR, BZR-T33 and NCI-H1299 cells).

Fhit regulates cell–cell adhesion in lung tumor cells

To explore the potential role of Fhit during tumor cell invasion, we chose NCI-H1299 cells as a model of Fhit-negative highly invasive tumor cells and HBE4-E6/E7 cells as a model of Fhit-positive poorly invasive tumor cells to, respectively, induce Fhit expression by stable transfection of *Fhit* cDNA and inhibit Fhit expression by transient transfection of *Fhit* small interfering RNA (siRNA).

At first, we observed that Fhit overexpression in NCI-H1299 and Fhit inhibition in HBE4-E6/E7 induced morphological modifications (Figure 3a). NCI-H1299-Fhit cells showed a more cohesive and epithelioid phenotype than NCI-H1299-mock cells. Conversely, HBE4-E6/E7 transfected with *Fhit* siRNA were less cohesive and showed lamellipodium-type extensions characteristic of a migratory phenotype compared with HBE4-E6/E7 transfected with the corresponding scrambled siRNA. In addition, we showed by immunocytochemistry that the modulation of Fhit expression

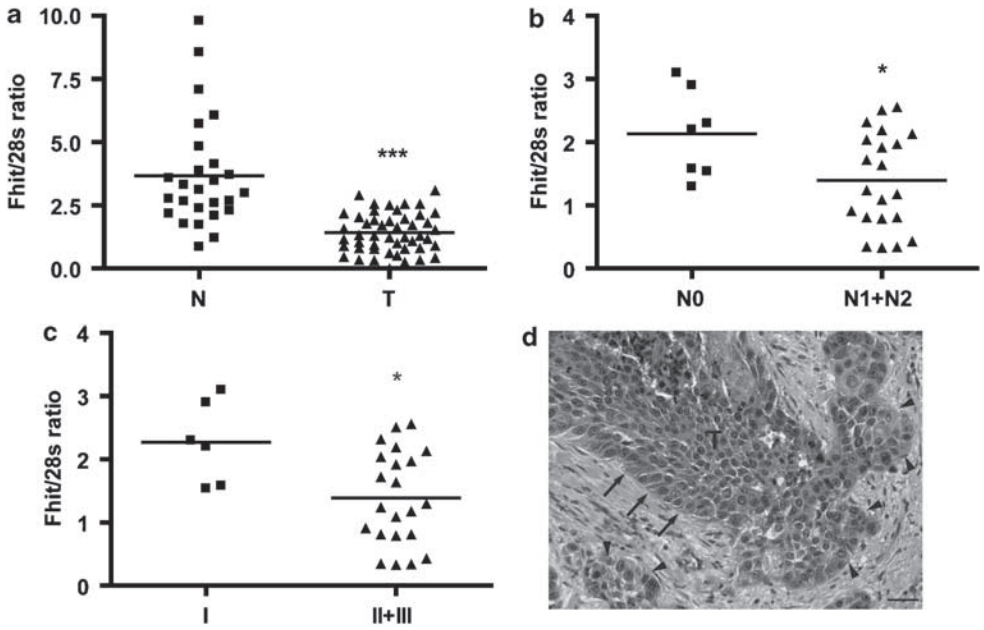

Figure 1 Loss of fragile histidine triad (Fhit) expression is associated with tumor invasion in non-small cell lung carcinomas. Analysis of *Fhit* mRNA levels by semiquantification of RT–PCR analysis of Fhit normalized on the basis of 28S rRNA values in normal and tumor tissues (**a**), according to the node (N) status of squamous-cell carcinomas (**b**), and according to the tumor–node–metastasis classification of squamous-cell carcinomas (**c**). Data are expressed as medians relative to each group of tissues. The Fhit protein was detected by immunohistochemistry in a squamous-cell carcinoma. Although Fhit was expressed by tumor cells still delimited by the basement membrane (arrows), the Fhit staining was lost in tumor cells located at the invading front of the tumor cluster (T), where the basement membrane was disrupted (arrowheads). Bar, 56 μm (**d**). $*P<0.05$; $***P<0.001$.

influenced the subcellular localization of molecules implicated in tight and adherens junctions (Figure 3b). We observed a higher expression of occludin, ZO-1 and β-catenin at the cell membrane in NCI-H1299-Fhit cells compared with NCI-H1299-mock cells, essentially showing a cytoplasmic expression of these adhesion molecules. E-cadherin was not expressed by NCI-H1299 cells and no change was detected when Fhit expression was induced. In contrast, occludin, ZO-1, E-cadherin and β-catenin were delocalized from the cell membrane towards the cytoplasm and/or the nucleus of *Fhit*-siRNA HBE4-E6/E7 transfected cells compared with control cells. As shown by the western blot analysis, total level of the cell junctional proteins were found unchanged with the exception of β-catenin, which was up-regulated in NCI-H1299-Fhit cells (Figure 3c).

Fhit regulates migration and invasion of lung tumor cells

As the modification of Fhit expression affected cell morphology and cell–cell adhesion, the effect of induction and repression of Fhit expression was tested on the cell behavior in a two-dimensional (2D) and a three-dimensional (3D) migration assay. In the 2D migration assay, trajectories of NCI-H1299-Fhit cells were shorter and migration speed was significantly reduced compared with mock cells (5.24 ± 0.84 and 11.73 ± 0.64 μm/h, respectively) ($P<0.05$) (Figure 4a). Trajectories of HBE4-E6/E7 transfected with *Fhit* siRNA were on the contrary longer and their migration speed was significantly increased compared with control cells (19.30 ± 2.71 and 15.19 ± 0.97 μm/h, respectively)

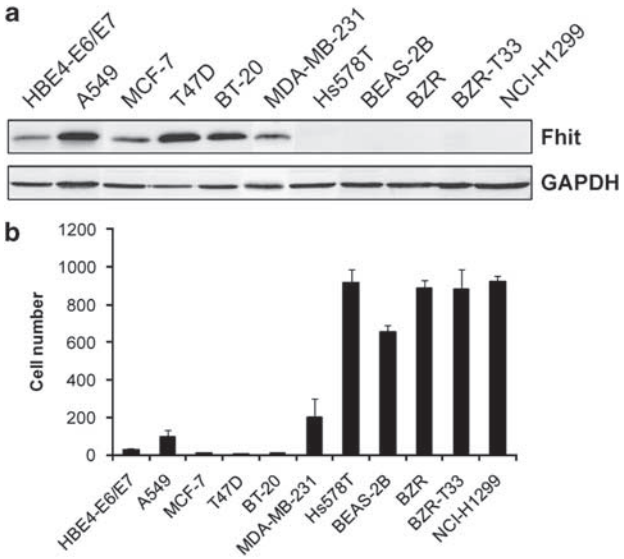

Figure 2 Loss of fragile histidine triad (Fhit) expression is associated with *in vitro* cell invasion. (**a**) The level of Fhit expression was evaluated by western blot analysis in HBE4-E6/E7, A549, MCF-7, T47D, BT-20, MDA-MB-231, Hs578T, BEAS-2B, BZR, BZR-T33 and NCI-H1299 cell lines. (**b**) The invasive capacities of the lung and mammary cell lines were tested in a modified Boyden chamber assay.

($P<0.05$) (Figure 4a). In the 3D migration assay, as compared with their corresponding control, the induction of Fhit in NCI-H1299 cells and the inhibition of Fhit in HBE4-E6/E7 cells resulted in a lower (4.47 ± 0.37 versus 6.60 ± 0.32 μm/h) ($P<0.05$) and a

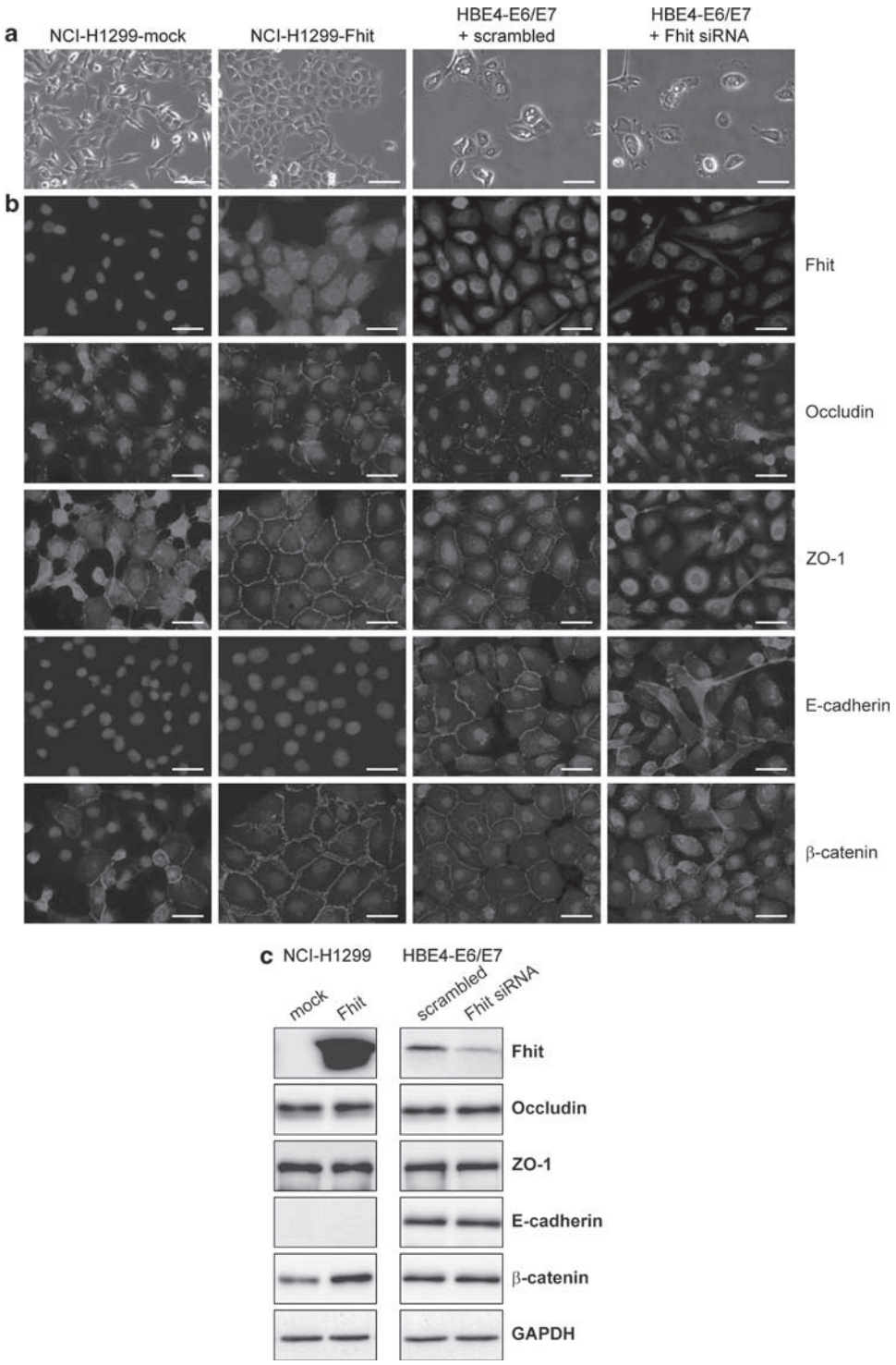

Figure 3 Fragile histidine triad (Fhit) regulates cell–cell adhesion in lung tumor cells. (**a**) Phase-contrast photographs showing the morphology of NCI-H1299 cells transfected with empty vector (NCI-H1299-mock) or *Fhit* cDNA (NCI-H1299-Fhit) and HBE4-E6/E7 cells transfected with scrambled siRNA (HBE4-E6/E7 + scrambled) or *Fhit* siRNA (HBE4-E6/E7 + *Fhit* siRNA). Bar, 106 μm for NCI-H1299 cells and 53 μm for HBE4-E6/E7 cells. (**b**) Immunofluorescence analysis of Fhit, occludin, ZO-1, E-cadherin and β-catenin expression in NCI-H1299 and HBE4-E6/E7 transfectants. Nuclei were counterstained with Dapi. Bars, 37 μm. (**c**) Western blot analysis of protein levels of Fhit and cell–cell adhesion molecules in NCI-H1299 cells transfected with empty vector (NCI-H1299-mock) or *Fhit* cDNA (NCI-H1299-Fhit) and HBE4-E6/E7 cells transfected with scrambled siRNA (HBE4-E6/E7 + scrambled) or *Fhit* siRNA (HBE4-E6/E7 + *Fhit* siRNA). The levels of glyceraldehyde-3-phosphate dehydrogenase served as loading controls.

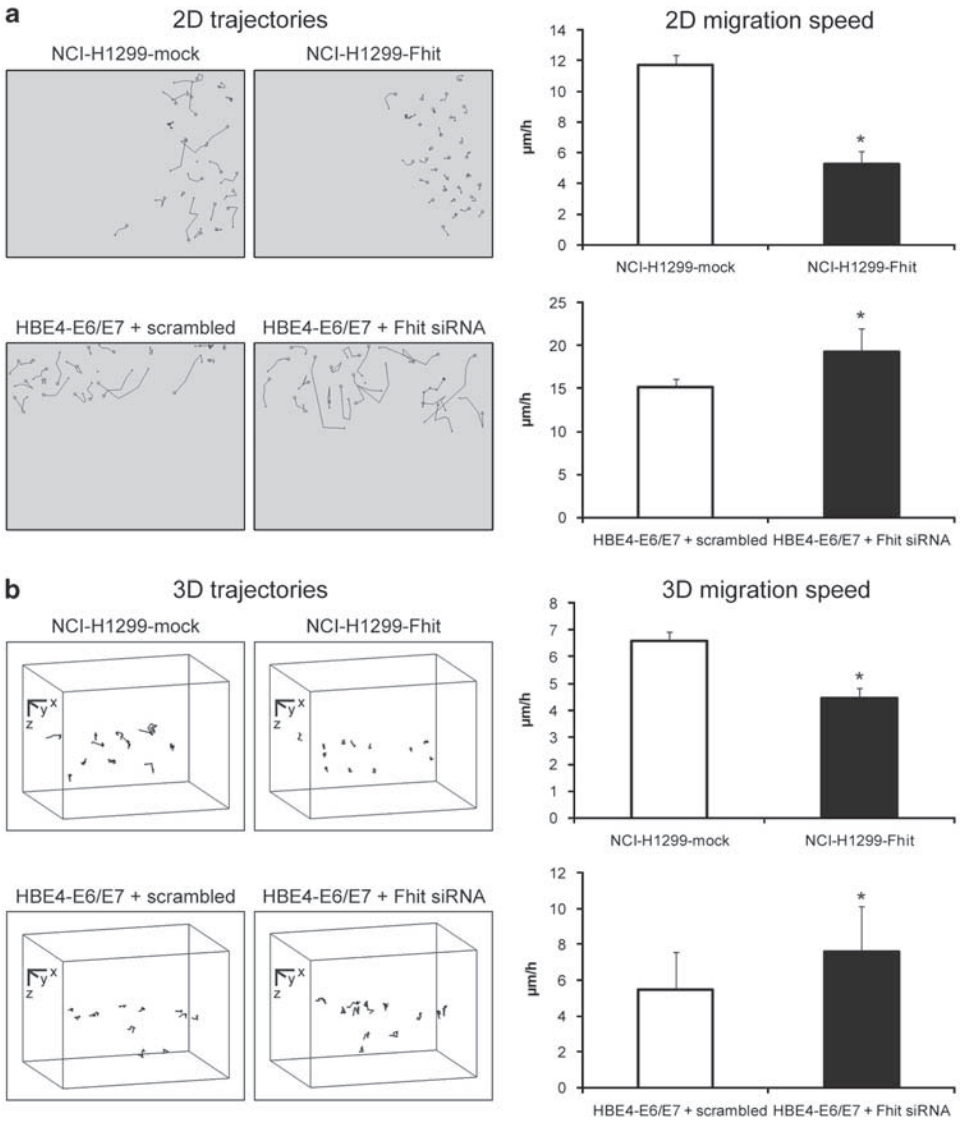

Figure 4 Fragile histidine triad (Fhit) regulates the migration of lung tumor cells. (**a**) Comparison of trajectories and migration speeds of NCI-H1299 cells transfected with empty vector (NCI-H1299-mock) or *Fhit* cDNA (NCI-H1299-Fhit) and HBE4-E6/E7 cells transfected with scrambled siRNA (HBE4-E6/E7 + scrambled) or *Fhit* siRNA (HBE4-E6/E7 + *Fhit* siRNA) in a 2D migration assay. (**b**) Comparison of trajectories and migration speeds along the *x*–*y*–*z* plane of NCI-H1299 and HBE4-E6/E7 transfectants in a 3D migration assay. $^*P<0.05$.

higher migration speed (7.62 ± 2.53 versus 5.47 ± 2.12 μm/h) ($P<0.05$), respectively (Figure 4b).

The invasive capacities of different transfected cells were also tested in a modified Boyden chamber assay. The NCI-H1299-Fhit transfectants were less invasive than the mock transfectants (1056 ± 213 versus 3524 ± 1025 invading cells) ($P<0.05$) (Figure 5a), whereas the *Fhit*-siRNA HBE4-E6/E7 transfectants were more invasive than the scrambled siRNA HBE4-E6/E7 transfectants (1585 ± 148 versus 508 ± 266 invading cells) ($P<0.05$) (Figure 5b). Involvement of Fhit in cell invasion regulation was also observed in other lung and mammary cell lines by using a modified Boyden chamber assay (Supplementary Figure). We also showed that incubation with the synthetic MMP inhibitor GM6001 induced a dose-dependent decrease in the invasive capacities of HBE4-E6/E7 transfected with *Fhit* siRNA (25 μM GM6001: 559 ± 226 invading cells, 50 μM GM6001: 198 ± 102 invading cells and 100 μM GM6001: 98 ± 94 invading cells) ($P<0.05$), thus demonstrating that this process was MMP-dependent (Figure 5b).

Fhit regulates MMP and vimentin expression in lung tumor cells

As the modification of Fhit expression influenced the cell migratory and invasive behavior in an MMP-dependent manner, we investigated the role of Fhit in the regulation of MMP expression. We observed by RT–PCR analysis that NCI-H1299-Fhit cells expressed less MMP-2 (0.63 ± 0.09-fold) ($P<0.05$) and MMP-9 (0.52 ± 0.16-fold) ($P<0.05$) mRNA and that HBE4-E6/E7 cells transfected with *Fhit* siRNA expressed more MMP-2 (1.73 ± 0.61-fold) ($P<0.05$) and MMP-9

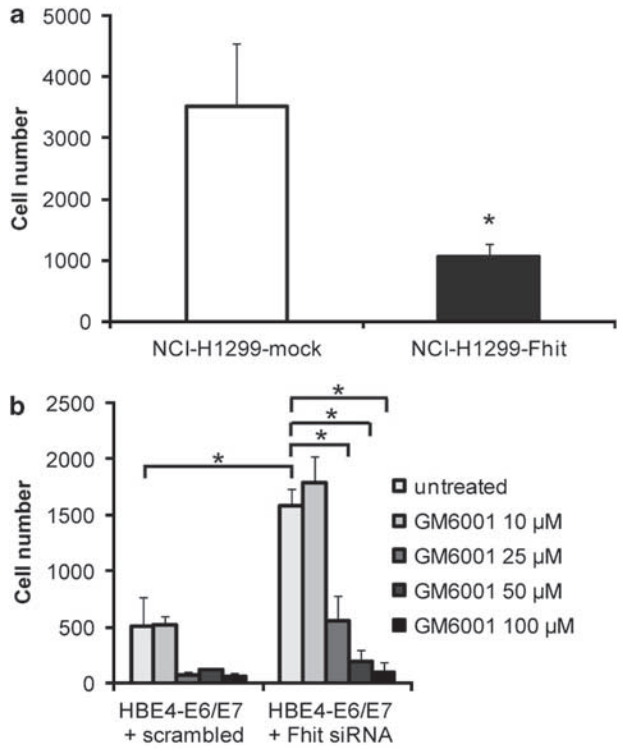

Figure 5 Fragile histidine triad (Fhit) regulates invasion of lung tumor cells. (**a**) Comparison of the invasive properties of NCI-H1299 cells transfected with empty vector (NCI-H1299-mock) or *Fhit* cDNA (NCI-H1299-Fhit) using a modified Boyden chamber assay. (**b**) Comparison of the invasive properties of HBE4-E6/E7 cells transfected with scrambled siRNA (HBE4-E6/E7 + scrambled) or *Fhit* siRNA (HBE4-E6/E7 + *Fhit* siRNA) using a modified Boyden chamber assay. A specific synthetic matrix metalloproteinase (MMP) inhibitor, GM6001, was used to show that Fhit inhibition induces invasion in an MMP-dependent manner. $^*P<0.05$.

$(7.55 \pm 3.77$-fold) ($P<0.05$) mRNA than their respective controls (Figure 6a). Zymography analysis allowed us to detect a downregulation of both pro- and active forms of MMP-2 (0.26 ± 0.08-fold) ($P<0.05$) and MMP-9 (0.36 ± 0.09-fold) ($P<0.05$) proteins in NCI-H1299 cells after induction of Fhit expression (Figure 6b). On the contrary, both the pro- and active forms of MMP-2 (2.3 ± 1.4-fold) ($P<0.05$) and MMP-9 (7.3 ± 5.8-fold) ($P<0.01$) enzymes were upregulated in *Fhit*-siRNA HBE4-E6/E7 transfectants (Figure 6b). MT1-MMP was also found to be upregulated at the mRNA (2.62 ± 1.05-fold) ($P<0.05$) and protein level (2.67 ± 1.87-fold) ($P<0.05$) after Fhit inhibition in HBE4-E6/E7 cells as shown by RT–PCR (Figure 6a) and western blot (Figure 6c) analyses, respectively. Furthermore, the quantitative determination of active MT1-MMP revealed a 1.8 ± 0.09-fold increase of MT1-MMP activity in *Fhit*-siRNA HBE4-E6/E7 transfectants compared with control transfectants ($P<0.05$) (Figure 6d). MT1-MMP was not expressed by NCI-H1299 cells (data not shown). We also searched for a potential regulation of the type III intermediate filament vimentin, known to be implicated in cell migration and EMT process. Whereas no regulation of vimentin was observed in NCI-H1299-Fhit transfectants (data not shown), a significant increase of vimentin was shown in *Fhit*-siRNA HBE4-E6/E7 transfectants both at the mRNA (3.48 ± 0.78-fold) ($P<0.05$) and at the protein level (2.15 ± 0.59-fold) ($P<0.01$), as shown by RT–PCR (Figure 6a) and western blotting (Figure 6c), respectively.

Discussion

In this study, we show that Fhit controls the invasive phenotype of lung tumor cells. We indeed showed that (a) a low Fhit expression is correlated with tumor invasion *in vivo* and *in vitro*, (b) Fhit regulates cell–cell adhesion, (c) Fhit regulates cell migration and invasion, and (d) Fhit regulates MMP and vimentin expression.

We first found that Fhit expression is reduced in human lung carcinoma samples compared with normal lung tissue. This may be attributed to the role of *Fhit* as a tumor suppressor gene (Pekarsky *et al*., 2002). Moreover, its downregulation is correlated with tumor aggressiveness according to the lymph node status and the TNM stage of squamous-cell carcinomas. We also observed that Fhit expression is lost at the invading front of tumor clusters of lung carcinomas. Even though Fhit inactivation has been shown to be frequently detected in preinvasive bronchial lesions (Sozzi *et al*., 1998; Pekarsky *et al*., 2002), these data, along with previous studies showing a link with poor differentiation, lymph node metastasis and poor survival (Pylkkanen *et al*., 2002; Maruyama *et al*., 2004; Nakata *et al*., 2006), clearly suggest its involvement in later stages of lung tumor progression. This is in agreement with our *in vitro* data showing a lack of Fhit expression in highly invasive lung and mammary tumor cell lines. Taken together, these *in vivo* and *in vitro* results suggest that Fhit inactivation, in addition to its role in tumorigenesis, is implicated in tumor invasion. In the same way, some genes such as E-cadherin also have dual functions in tumor progression as a tumor suppressor and a tumor invasion regulator (Van Aken *et al*., 2001).

Accordingly, we showed that overexpression of Fhit in a highly invasive NCI-H1299 lung cell line and inhibition of Fhit expression in a poorly invasive HBE4-E6/E7 lung cell line, respectively, induce a decrease and an increase in their migratory and invasive capacities. Furthermore, the cell invasion induced by Fhit inhibition was MMP-dependent. Concomitantly with these modifications of cell behavior, we also observed changes in subcellular localization of tight and adherens junction molecules and a regulation of MMP and vimentin expression. Indeed, NCI-H1299-Fhit transfectants express more occludin, ZO-1 and β-catenin at the cell membrane and less MMP-2 and -9 than the control cells. On the contrary, a loss of occludin, ZO-1, E-cadherin and β-catenin at cell–cell contacts and an upregulation of MMP-2, MMP-9 as well as MT1-MMP and vimentin expression were seen in *Fhit*-siRNA-transfected HBE4-E6/E7 cells. All these molecules

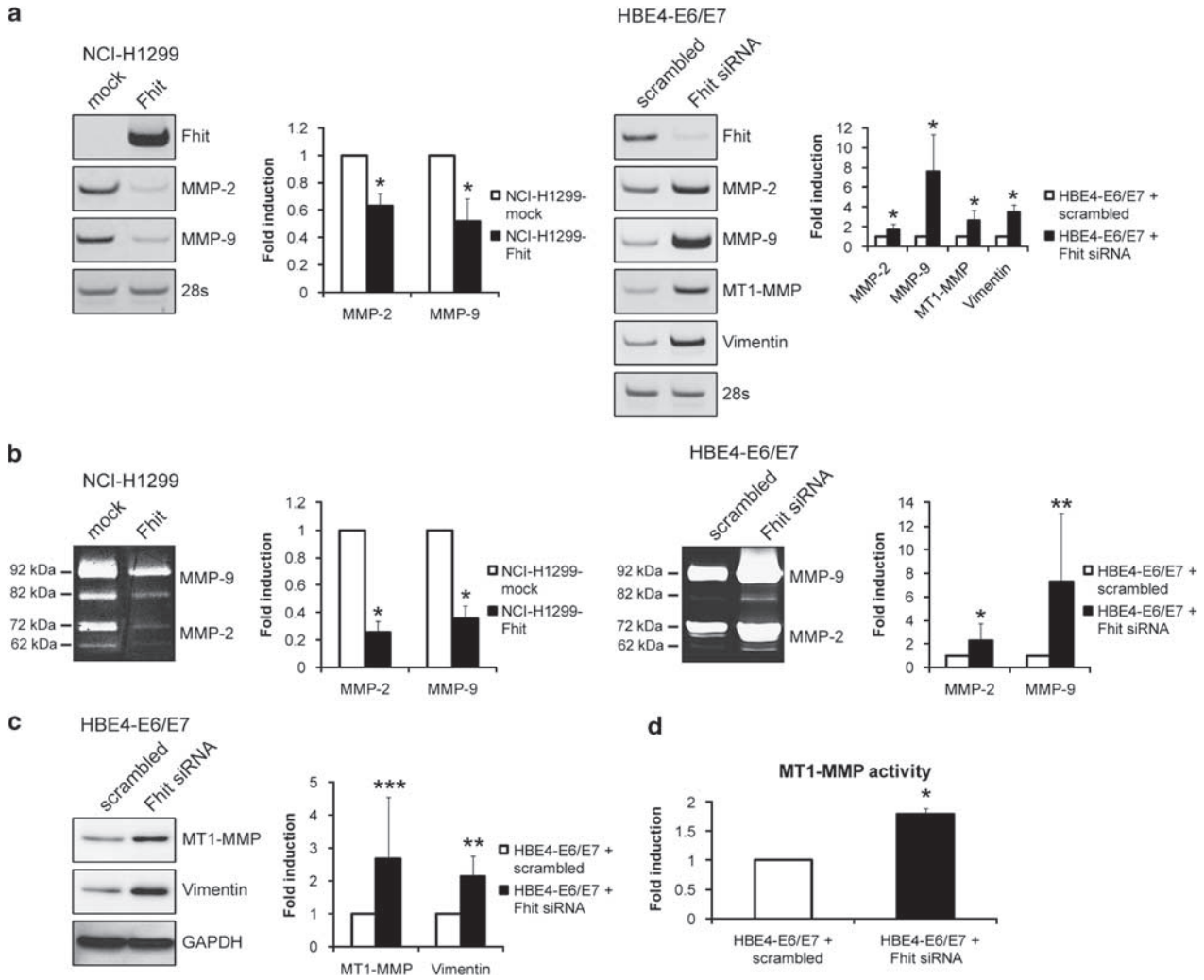

Figure 6 Fragile histidine triad (Fhit) regulates matrix metalloproteinase (MMP) and vimentin expression in lung tumor cells. (**a**) RT–PCR analysis of Fhit, MMP-2 and MMP-9 mRNA levels in NCI-H1299 cells transfected with empty vector (NCI-H1299-mock) or *Fhit* cDNA (NCI-H1299-Fhit) and of Fhit, MMP-2, MMP-9, MT1-MMP and vimentin mRNA levels in HBE4-E6/E7 cells transfected with scrambled siRNA (HBE4-E6/E7 + scrambled) or *Fhit* siRNA (HBE4-E6/E7 + *Fhit* siRNA) normalized with the 28S rRNA values. Data are expressed as fold induction relative to the respective controls. (**b**) Zymography analyses of gelatinolytic activities (92 kDa, pro-MMP-9; 82 kDa, active MMP-9; 72 kDa, pro-MMP-2; 62 kDa, active MMP-2) in conditioned media of NCI-H1299 and HBE4-E6/E7 transfectants. Data are expressed as fold induction relative to the respective controls. (**c**) Western blot analysis of MT1-MMP and vimentin protein levels normalized with GAPDH in HBE4-E6/E7 transfectants. Data are expressed as fold induction relative to the control cells. (**d**) MT1-MMP activity analysis in HBE4-E6/E7 transfectants. Data are expressed as fold induction relative to the control cells. $*P<0.05$; $**P<0.01$; $***P<0.001$.

demonstrated here as regulated by Fhit are known to have key functions in tumor invasion associated with EMT (Polette *et al*., 2004, 2007; Lee *et al*., 2006; Gavert and Ben Ze'ev, 2007, 2008).

Even though the mechanisms by which Fhit could regulate EMT in these lung tumor cells remain largely unknown, its ability to reorganize cell–cell adhesion complexes could directly contribute to the modulation of EMT target molecules such as MMPs and vimentin. Interestingly, the reexpression of E-cadherin has been described to repress MMP expression in invasive cancer cells, likely through inhibition of the β-catenin TCF/LEF signaling pathway (Luo *et al*., 1999; Nawrocki-Raby *et al*., 2003). Indeed, MT1-MMP has been proven to be a target of the β-catenin/TCF complex as well as MMP-7 and MMP-26 (Brabletz *et al*., 1999; Crawford *et al*., 1999; Marchenko *et al*., 2002; Takahashi *et al*., 2002). Moreover, MMP-1, MMP-3 and MMP-9 constitute potential targets of β-catenin/TCF, because their promoters contain TCF-binding sites. ZO-1 regulates MT1-MMP expression in human breast cancer cells and the activation of the MT1-MMP promoter by ZO-1 is associated with the activation of the β-catenin TCF/LEF signaling pathway (Polette *et al*., 2005). Finally, it has been shown that the vimentin promoter is also a target of the β-catenin/TCF pathway (Gilles *et al*., 2003). Therefore, the mechanism by which Fhit suppresses tumor invasion in these cells may involve the β-catenin TCF/LEF signaling pathway. In accordance with this hypothesis, Weiske *et al*. (2007) have shown that Fhit is a repressor of β-catenin transcriptional activity. Fhit is indeed able to associate with the LEF1/

TCF/β-catenin complex by directly binding to β-catenin and to repress promoter activation of target genes such as cyclin D1, axin 2, survivin and MT1-MMP (Weiske *et al*., 2007). However, we described here a regulation of MMP-2 expression by Fhit. To our knowledge, the MMP-2 promoter does not contain any TCF-binding site. All these data further suggest that Fhit may engage another or several signaling pathways to regulate the invasive phenotype of these tumor cells. In particular, Fhit has also been shown to downregulate NF-κB as well as PI3K–Akt–survivin and Ras/Rho GTPase signaling pathways and to be a target of the protein kinase Src (Pekarsky *et al*., 2004; Nakagawa and Akao, 2006; Semba *et al*., 2006; Jayachandran *et al*., 2007).

In conclusion, this study shows that Fhit controls the invasive phenotype of lung tumor cells by regulating several EMT key events such as cell–cell adhesion and MMP and vimentin expression. Taken together with our data showing the regulation of the invasiveness of several lung and mammary cell lines by Fhit, these results suggest a general mechanism of control of tumor invasion by Fhit. Thus, this study highlights a dual role for Fhit during cancer progression. Besides its tumor suppressive function, *Fhit* is also a tumor invasion suppressor gene. This study therefore reinforces the usefulness of Fhit detection as a prognostic marker and of *Fhit* gene therapy for the treatment of cancer.

Materials and methods

Tumor tissue samples

Surgically resected tumors were collected after obtaining informed consent from 48 patients with primary NSCLC (28 squamous-cell carcinomas and 20 adenocarcinomas) of stages I (15 cases), II (19 cases) and III (14 cases) according to the TNM classification. A total of 26 normal lung tissues matching the tumor samples were also collected.

Tumor cell lines

Human lung HBE4-E6/E7, A549, BEAS-2B, NCI-H1299 and BZR and mammary T47D, MCF-7, BT-20, MDA-MB-231 and Hs578T cell lines were obtained from the American Type Culture Collection (Rockville, MD, USA). BZR-T33 lung cells were provided by Curtis C Harris (National Cancer Institute, Bethesda, MD, USA). A549, BEAS-2B, BZR, BZR-T33, T47D, MCF-7, BT-20, MDA-MB-231 and Hs578T were cultured in DMEM (Gibco, Invitrogen, Carlsbad, CA, USA) containing 10% fetal calf serum (FCS) (Gibco), and NCI-H1299 in RPMI (Gibco) containing 10% FCS and HBE4-E6/E7 in Keratinocyte-SFM (Gibco) supplemented with 0.2 ng/ml EGF and 25 μg/ml BPE.

Stable transfection of Fhit expression vector

The eukaryotic expression plasmid pcDNA3.1/Zeo (−)-Fhit expressing the *Fhit* cDNA was constructed by subcloning the *Xho*I/*Hin*dIII fragment from the pUSEamp(−)-Fhit plasmid (Upstate Biotechnology, Lake Placid, NY, USA) into the pcDNA3.1/Zeo (−) vector (Invitrogen). NCIH-1299 cells were stably transfected with the pcDNA3.1/Zeo (−)-*Fhit* plasmid or the pcDNA3.1/Zeo (−) empty vector by electroporation. The transfected populations were subjected to a selective pressure with zeocin.

Transfection of siRNA

Three *Fhit* specific sequences were selected in the coding sequence of *Fhit* (GeneBank accession number: NM_002012) to generate 21-nucleotide sense and 21-nucleotide antisense strands of the type (19N) TT (N, any nucleotide). The selected 19-nt sequences were as follows: *Fhit* si1, 5′-CAUCUCAUCA AGCCCUCUG-3′; *Fhit* si2, 5′-GGAAGGCUGGAGACUU UCA-3′; and *Fhit* si3 5′-GGAGGACUUUCCUGCCUCU-3′ (Eurogentec, Seraing, Belgium). Three corresponding scrambled duplexes that do not recognize any sequence in the human genome were used as controls. A total of 100 000 HBE4-E6/E7 cells were transfected with a mix of the three siRNA duplexes (20 nM) by calcium phosphate-precipitation method as previously described (Polette *et al*., 2005). Supernatants and cells cultured for 24 h without BPE were then harvested for zymography, RT–PCR and western blot analyses.

RT–PCR analysis

RNA was extracted from normal and tumor lung tissues frozen in liquid nitrogen with the RNA Easy Qiagen kit (Qiagen, MD, USA) and from NCI-H1299 and HBE4-E6/E7 transfectants with the High Pure RNA isolation kit (Roche Diagnostics GmbH, Mannheim, Germany). Forward and reverse primers (Eurogentec) for human *Fhit*, MT1-MMP, MMP-2, MMP-9, vimentin and 28S rRNA were designed as follows: *Fhit* primers (forward 5′-GCTTCCATGACCTGCGT CCTGAT-3′, reverse 5′-GCTGTCATTCCTGTGAAAGTCT CC-3′), MMP-2 primers (forward 5′-AGATCTTCTTCTT CAAGGA CCGGTT-3′, reverse 5′-GGCTGGTCAGTGGCT TGGGGTA-3′), MMP-9 primers (forward 5′-GCGGAGATT GGGAACCAGGTGTA -3′, reverse 5′-GACGCGCCTGTGT ACACCCACA-3′), MT1-MMP primers (forward 5′-GGATA CCCAATGCCCATTGGCCA-3′, reverse 5′-CCATTGGGCA TCCAGAAGAGAC-3′), vimentin primers (forward 5′-GACA ATGCGTCTCTGGCACGTCTT-3′, reverse 5′-TCCTCCGC CTCCTGCAGGTTCTT-3′), and 28S primers (forward 5′-GT TCACC CACTAATAGGGAACGTGA-3′, reverse 5′-GGAT TCTGACTTAGAGGCGTTCAGT-3′). RT–PCR was performed by using the Thermostable r*Tth* Reverse Transcriptase RNA PCR kit (Applied Biosystem, Foster City, CA, USA) as previously described (Polette *et al*., 2005).

Immunohistochemistry

Immunohistochemistry for Fhit was carried out on paraffin serial sections. After antigen retrieval pretreatment in citrate buffer, slides were incubated with a rabbit polyclonal antiboby to Fhit (1:200) (ZR44; Zymed, Invitrogen). Subsequent steps were performed with the LSAB+ system-AP kit (Dako, Carpinteria, CA, USA). Alkaline phosphatase activity was revealed with fuschin + substrate-chromogen (Dako). Slides were counterstained with Mayer's haematoxylin.

Immunofluorescence

Subconfluent monolayers of NCI-H1299 and HBE4-E6/E7 transfectants cultured on glass coverslips were fixed with methanol or paraformaldehyde for analysis of adhesion molecules or Fhit, respectively. The coverslips were incubated with a mouse monoclonal antibody against occludin (1:25) (clone OC-3F10, Zymed), a mouse monoclonal antibody against ZO-1 (1:25) (clone ZO1-1A12, Zymed), a mouse monoclonal antibody against E-cadherin (1:100) (clone 36, BD Transduction Laboratories, BD Biosciences, San Jose, CA, USA), a mouse monoclonal antibody against β-catenin (1:500) (clone 14, BD Transduction Laboratories) or a rabbit polyclonal antibody against Fhit (1:25) (ZR44). Monolayers

were next incubated with Alexa Fluor 594-coupled anti-mouse or anti-rabbit IgG (1:200) (Molecular Probes, Eugene, OR, USA). Nuclei were stained with Dapi (Molecular Probes).

Western blotting
Total proteins were extracted in radioimmunoprecipitation assay buffer containing a complete protease inhibitor cocktail (Roche Diagnostics GmbH). Proteins were separated on SDS–PAGE gels and transferred to a polyvinylidene difluoride membrane (NEN, Boston, MA, USA). The membranes were incubated with either a rabbit polyclonal antibody to Fhit (1:250) (ZR44) or mouse monoclonal antibodies to MT1-MMP (1:1000) (clone 2D7, provided by Dr Rio, IGBMC, Illkirch, France), vimentin (1:1000) (clone V9, Dako), occludin (1:1000) (clone OC-3F10), ZO-1 (1:1000) (clone ZO1-1A12), E-cadherin (1:2500) (clone 36) and β-catenin (1:5000) (clone 14). The following steps were performed as previously described (Polette *et al*., 2005). Subsequent detection of glyceraldehyde-3-phosphate dehydrogenase (GAPDH) (using a mouse antibody, 1:300, clone 6C5, Chemicon, Millipore, Billerica, MA, USA) was performed on the same filters as a control.

2D migration assay
For each cell type, 5×10^4 cells were seeded inside a restriction glass ring. After 48 h, the ring was removed to induce cell migration. After 24 h, cell migration analysis was performed using an inverted microscope (Axiovert 200, Zeiss, Oberkochen, Germany) equipped with an environmental chamber (Incubator XL-3, Pecon, Erbach, Germany) with 5% CO_2 in air at 37 °C and a charge-coupled device camera (Coolsnap, Roper Scientific, Photometrics, Tucson, AZ, USA) and driven by the Axiovision software (Zeiss). Image sequences of the cells were recorded every 15 min for 6 h at $\times 20$ magnification and the trajectories and the migration speeds were analysed with a software developed in our laboratory (Zahm *et al*., 1997).

3D migration assay
A two-layer type-I collagen gel was prepared on Transwell (Corning Incorporated, Corning, NY, USA). A total of 2.5×10^4 cells were incorporated in the second collagen gel layer. Cell migration analysis was performed using the same microscope and camera as for 2D migration assay. Image sequences of the cells within the collagen gel were recorded every hour at 150 successive Z levels (3 μm between each depth level) at $\times 10$ magnification. The migratory behavior of the cells was finally analysed by using a cell tracking software developed in our laboratory, which allows the 3D representation of the trajectories and the migration speed quantitation in *xy* and *z* planes (Hazgui *et al*., 2005).

Modified Boyden chamber invasion assay
The *in vitro* invasive properties of cells were assessed using a modified Boyden chamber assay. A total of 10^5 cells were placed in the upper compartment of the invasion chamber (BD BioCoat Matrigel Invasion Chamber, BD Biosciences, Bedford, MA, USA). For MMP inhibition experiments, the broad-spectrum synthetic MMP inhibitor GM6001 (Calbiochem, Merck Biosciences, Darmstadt, Germany) was added to the cells in the upper compartment of the insert (10–100 μM). The chambers were incubated for 24 h at 37 °C. The filters were then fixed in methanol and stained with haematoxylin. Quantification of the invasion assay was performed by counting the number of cells at the lower surface of the filters (23 fields at 400-fold magnification).

Gelatin zymography analysis
Supernatants of cells grown for 48 h in serum-free conditions were collected, centrifugated and separated on 10% polyacrylamide SDS gel containing 0.1% (w/v) gelatin. The gel was washed for 1 h at room temperature in a 2% (v/v) Triton X-100 solution, transferred to a 50 mM Tris-HCl/10 mM $CaCl_2$ (pH 7.6) buffer and incubated overnight at 37 °C. The gel was stained in a 0.1% (w/v) Coomassie Blue (G250)/45% (v/v) methanol/10% (v/v) acetic acid solution and de-stained in a 10% (v/v) acetic acid/20% (v/v) methanol solution.

MT1-MMP activity assay
Active MT1-MMP level was measured with the MMP-14 Biotrack Activity Assay System according to the manufacturer's instructions (Amersham, GE Healthcare, Buckinghamshire, UK).

Statistical analysis
Data are expressed as means ± standard deviation. The nonparametric Mann–Whitney *U*-test was used for statistical analyses. $P < 0.05$ was considered to be significant.

Conflict of interest

The authors declare no conflict of interest.

Acknowledgements

This study was supported by the Région Champagne-Ardenne, the Ligue Contre le Cancer (Comité de la Marne), the Lions Club of Soissons, Un Euro contre le Cancer and the Fond National pour la Santé ACI 2004–2010 INCa (Cancéropôle Grand-Est project).

References

Barnes LD, Garrison PN, Siprashvili Z, Guranowski A, Robinson AK, Ingram SW *et al*. (1996). Fhit, a putative tumor suppressor in humans, is a dinucleoside 5′,5‴-P1,P3-triphosphate hydrolase. *Biochemistry* **35**: 11529–11535.

Brabletz T, Jung A, Dag S, Hlubek F, Kirchner T. (1999). beta-Catenin regulates the expression of the matrix metalloproteinase-7 in human colorectal cancer. *Am J Pathol* **155**: 1033–1038.

Campiglio M, Bianchi F, Andriani F, Sozzi G, Tagliabue E, Menard S *et al*. (2006). Diadenosines as FHIT-ness instructors. *J Cell Physiol* **208**: 274–281.

Cavazzoni A, Petronini PG, Galetti M, Roz L, Andriani F, Carbognani P *et al*. (2004). Dose-dependent effect of FHIT-inducible expression in Calu-1 lung cancer cell line. *Oncogene* **23**: 8439–8446.

Chang C, Werb Z. (2001). The many faces of metalloproteases: cell growth, invasion, angiogenesis and metastasis. *Trends Cell Biol* **11**: S37–S43.

Crawford HC, Fingleton BM, Rudolph-Owen LA, Goss KJ, Rubinfeld B, Polakis P *et al*. (1999). The metalloproteinase matrilysin is a target of beta-catenin transactivation in intestinal tumors. *Oncogene* **18**: 2883–2891.

Dumon KR, Ishii H, Fong LY, Zanesi N, Fidanza V, Mancini R *et al*. (2001). *FHIT* gene therapy prevents tumor development in Fhit-deficient mice. *Proc Natl Acad Sci USA* **98**: 3346–3351.

Gavert N, Ben Ze'ev A. (2007). beta-Catenin signaling in biological control and cancer. *J Cell Biochem* **102**: 820–828.

Gavert N, Ben Ze'ev A. (2008). Epithelial–mesenchymal transition and the invasive potential of tumors. *Trends Mol Med* **14**: 199–209.

Gilles C, Polette M, Mestdagt M, Nawrocki-Raby B, Ruggeri P, Birembaut P *et al*. (2003). Transactivation of vimentin by beta-catenin in human breast cancer cells. *Cancer Res* **63**: 2658–2664.

Gilles C, Polette M, Piette J, Delvigne AC, Thompson EW, Foidart JM *et al*. (1996). Vimentin expression in cervical carcinomas: association with invasive and migratory potential. *J Pathol* **180**: 175–180.

Gilles C, Polette M, Zahm JM, Tournier JM, Volders L, Foidart JM *et al*. (1999). Vimentin contributes to human mammary epithelial cell migration. *J Cell Sci* **112**(Part 24): 4615–4625.

Gilles C, Thompson EW. (1996). The epithelial to mesenchymal transition and metastatic progression in carcinoma. *Breast J* **2**: 83–96.

Hazgui S, Bonnet N, Cutrona J, Nawrocki-Raby B, Polette M, Chouchane L *et al*. (2005). 3D culture model and computer-assisted videomicroscopy to analyze migratory behavior of noninvasive and invasive bronchial epithelial cells. *Am J Physiol Cell Physiol* **289**: C1547–C1552.

Hendrix MJ, Seftor EA, Seftor RE, Trevor KT. (1997). Experimental co-expression of vimentin and keratin intermediate filaments in human breast cancer cells results in phenotypic interconversion and increased invasive behavior. *Am J Pathol* **150**: 483–495.

Huebner K, Croce CM. (2003). Cancer and the FRA3B/FHIT fragile locus: it's a HIT. *Br J Cancer* **88**: 1501–1506.

Ishii H, Dumon KR, Vecchione A, Fong LY, Baffa R, Huebner K *et al*. (2001). Potential cancer therapy with the fragile histidine triad gene: review of the preclinical studies. *JAMA* **286**: 2441–2449.

Jayachandran G, Sazaki J, Nishizaki M, Xu K, Girard L, Minna JD *et al*. (2007). Fragile histidine triad-mediated tumor suppression of lung cancer by targeting multiple components of the Ras/Rho GTPase molecular switch. *Cancer Res* **67**: 10379–10388.

Ji L, Fang B, Yen N, Fong K, Minna JD, Roth JA. (1999). Induction of apoptosis and inhibition of tumorigenicity and tumor growth by adenovirus vector-mediated fragile histidine triad (*FHIT*) gene overexpression. *Cancer Res* **59**: 3333–3339.

Lee JM, Dedhar S, Kalluri R, Thompson EW. (2006). The epithelial–mesenchymal transition: new insights in signaling, development, and disease. *J Cell Biol* **172**: 973–981.

Luo J, Lubaroff DM, Hendrix MJ. (1999). Suppression of prostate cancer invasive potential and matrix metalloproteinase activity by E-cadherin transfection. *Cancer Res* **59**: 3552–3556.

Marchenko GN, Marchenko ND, Leng J, Strongin AY. (2002). Promoter characterization of the novel human matrix metalloproteinase-26 gene: regulation by the T-cell factor-4 implies specific expression of the gene in cancer cells of epithelial origin. *Biochem J* **363**: 253–262.

Maruyama R, Sugio K, Yoshino I, Maehara Y, Gazdar AF. (2004). Hypermethylation of FHIT as a prognostic marker in nonsmall cell lung carcinoma. *Cancer* **100**: 1472–1477.

Nakagawa Y, Akao Y. (2006). Fhit protein inhibits cell growth by attenuating the signaling mediated by nuclear factor-kappaB in colon cancer cell lines. *Exp Cell Res* **312**: 2433–2442.

Nakata S, Sugio K, Uramoto H, Oyama T, Hanagiri T, Morita M *et al*. (2006). The methylation status and protein expression of CDH1, p16(INK4A), and fragile histidine triad in nonsmall cell lung carcinoma: epigenetic silencing, clinical features, and prognostic significance. *Cancer* **106**: 2190–2199.

Nawrocki-Raby B, Gilles C, Polette M, Martinella-Catusse C, Bonnet N, Puchelle E *et al*. (2003). E-Cadherin mediates MMP down-regulation in highly invasive bronchial tumor cells. *Am J Pathol* **163**: 653–661.

Negrini M, Monaco C, Vorechovsky I, Ohta M, Druck T, Baffa R *et al*. (1996). The *FHIT* gene at 3p14.2 is abnormal in breast carcinomas. *Cancer Res* **56**: 3173–3179.

Ohta M, Inoue H, Cotticelli MG, Kastury K, Baffa R, Palazzo J *et al*. (1996). The *FHIT* gene, spanning the chromosome 3p14.2 fragile site and renal carcinoma-associated t(3;8) breakpoint, is abnormal in digestive tract cancers. *Cell* **84**: 587–597.

Pace HC, Garrison PN, Robinson AK, Barnes LD, Draganescu A, Rosler A *et al*. (1998). Genetic, biochemical, and crystallographic characterization of Fhit-substrate complexes as the active signaling form of Fhit. *Proc Natl Acad Sci USA* **95**: 5484–5489.

Pekarsky Y, Garrison PN, Palamarchuk A, Zanesi N, Aqeilan RI, Huebner K *et al*. (2004). Fhit is a physiological target of the protein kinase Src. *Proc Natl Acad Sci USA* **101**: 3775–3779.

Pekarsky Y, Zanesi N, Palamarchuk A, Huebner K, Croce CM. (2002). *FHIT*: from gene discovery to cancer treatment and prevention. *Lancet Oncol* **3**: 748–754.

Polette M, Gilles C, Nawrocki-Raby B, Lohi J, Hunziker W, Foidart JM *et al*. (2005). Membrane-type 1 matrix metalloproteinase expression is regulated by zonula occludens-1 in human breast cancer cells. *Cancer Res* **65**: 7691–7698.

Polette M, Mestdagt M, Bindels S, Nawrocki-Raby B, Hunziker W, Foidart JM *et al*. (2007). Beta-catenin and ZO-1: shuttle molecules involved in tumor invasion-associated epithelial–mesenchymal transition processes. *Cells Tissues Organs* **185**: 61–65.

Polette M, Nawrocki-Raby B, Gilles C, Clavel C, Birembaut P. (2004). Tumour invasion and matrix metalloproteinases. *Crit Rev Oncol Hematol* **49**: 179–186.

Pylkkanen L, Wolff H, Stjernvall T, Tuominen P, Sioris T, Karjalainen A *et al*. (2002). Reduced Fhit protein expression and loss of heterozygosity at *FHIT* gene in tumours from smoking and asbestos-exposed lung cancer patients. *Int J Oncol* **20**: 285–290.

Reichert M, Muller T, Hunziker W. (2000). The PDZ domains of zonula occludens-1 induce an epithelial to mesenchymal transition of Madin-Darby canine kidney I cells. Evidence for a role of beta-catenin/Tcf/Lef signaling. *J Biol Chem* **275**: 9492–9500.

Roz L, Gramegna M, Ishii H, Croce CM, Sozzi G. (2002). Restoration of fragile histidine triad (FHIT) expression induces apoptosis and suppresses tumorigenicity in lung and cervical cancer cell lines. *Proc Natl Acad Sci USA* **99**: 3615–3620.

Seiki M. (2003). Membrane-type 1 matrix metalloproteinase: a key enzyme for tumor invasion. *Cancer Lett* **194**: 1–11.

Semba S, Trapasso F, Fabbri M, McCorkell KA, Volinia S, Druck T *et al*. (2006). Fhit modulation of the Akt-survivin pathway in lung cancer cells: Fhit-tyrosine 114 (Y114) is essential. *Oncogene* **25**: 2860–2872.

Siprashvili Z, Sozzi G, Barnes LD, McCue P, Robinson AK, Eryomin V *et al*. (1997). Replacement of Fhit in cancer cells suppresses tumorigenicity. *Proc Natl Acad Sci USA* **94**: 13771–13776.

Sozzi G, Pastorino U, Moiraghi L, Tagliabue E, Pezzella F, Ghirelli C *et al*. (1998). Loss of FHIT function in lung cancer and preinvasive bronchial lesions. *Cancer Res* **58**: 5032–5037.

Sozzi G, Veronese ML, Negrini M, Baffa R, Cotticelli MG, Inoue H *et al*. (1996). The *FHIT* gene 3p14.2 is abnormal in lung cancer. *Cell* **85**: 17–26.

Takahashi M, Tsunoda T, Seiki M, Nakamura Y, Furukawa Y. (2002). Identification of membrane-type matrix metalloproteinase-1 as a target of the beta-catenin/Tcf4 complex in human colorectal cancers. *Oncogene* **21**: 5861–5867.

Tobioka H, Isomura H, Kokai Y, Tokunaga Y, Yamaguchi J, Sawada N. (2004). Occludin expression decreases with the progression of human endometrial carcinoma. *Hum Pathol* **35**: 159–164.

Trapasso F, Krakowiak A, Cesari R, Arkles J, Yendamuri S, Ishii H *et al*. (2003). Designed FHIT alleles establish that Fhit-induced apoptosis in cancer cells is limited by substrate binding. *Proc Natl Acad Sci USA* **100**: 1592–1597.

Van Aken E, De Wever O, Correia da Rocha AS, Mareel M. (2001). Defective E-cadherin/catenin complexes in human cancer. *Virchows Arch* **439**: 725–751.

Weiske J, Albring KF, Huber O. (2007). The tumor suppressor Fhit acts as a repressor of beta-catenin transcriptional activity. *Proc Natl Acad Sci USA* **104**: 20344–20349.

Zahm JM, Kaplan H, Herard AL, Doriot F, Pierrot D, Somelette P *et al*. (1997). Cell migration and proliferation during the *in vitro* wound repair of the respiratory epithelium. *Cell Motil Cytoskeleton* **37**: 33–43.

Supplementary Information accompanies the paper on the Oncogene website (http://www.nature.com/onc)

Cells Tissues Organs

Cells Tissues Organs 2007;185:61–65
DOI: 10.1159/000101304

β-Catenin and ZO-1: Shuttle Molecules Involved in Tumor Invasion-Associated Epithelial-Mesenchymal Transition Processes

Myriam Polette[a] Mélanie Mestdagt[b] Sandrine Bindels[b]
Béatrice Nawrocki-Raby[a] Walter Hunziker[c] Jean-Michel Foidart[b]
Philippe Birembaut[a] Christine Gilles[b]

[a]INSERM UMRS 514, Laboratory of Histology, IFR 53, CHU Maison Blanche, Reims, France; [b]Laboratory of Developmental and Tumor Biology, University of Liège, CHU Sart-Tilman, B23, Liège, Belgium; [c]Institute of Molecular and Cell Biology, Epithelial Cell Biology Laboratory, Singapore, Singapore

Key Words
β-Catenin · ZO-1 · Vimentin · Matrix metalloproteinase · Epithelial-mesenchymal transition

Abstract
The cytoplasmic/nuclear relocalization of β-catenin and ZO-1 from the adherens and tight junctions are common processes of the epithelial-mesenchymal transition (EMT) associated with tumor invasion. Data are now accumulating to demonstrate that these molecules, which shuttle between the plasma membrane and the nucleus or the cytosol, are involved in signaling pathways, and contribute to the regulation of genes such as vimentin or matrix metalloproteinase-14 which are turned on during EMT.

Abbreviations used in this paper

EMT	epithelial-mesenchymal transition
MMP	matrix metalloproteinase
TCF/LEF	T cell factor/lymphoid enhancer factor
ZO-1	zonula occludens protein-1

The diminution of cell-cell adhesion is instrumental in the loss of epithelial features occurring in epithelial-mesenchymal transition (EMT) processes associated with the metastatic conversion of epithelial tumor cells. At the molecular level, this involves the reorganization of cell-cell adhesion complexes including adherens and tight junctions [Reichert et al., 2000; Ikenouchi et al., 2003; Thiery, 2003; Huber et al., 2005]. A reorganization of E-cadherin/catenins complexes has indeed been largely involved in EMT processes associated with epithelial cell migration in both physiological and pathological conditions. Such a reorganization also involves a relocalization of β-catenin, which in normal conditions participates in the linking of E-cadherin to the actin cytoskeleton [Wheelock and Johnson, 2003]. During EMT, β-catenin dissociates from the E-cadherin/catenin cell membrane complexes, accumulates in the cytoplasm and translocates into the nucleus where it acts as a transcriptional coactivator through its binding with the members of the T cell factor/lymphoid enhancer factor (TCF/LEF) transcription factor family [Harris and Peifer, 2005; Brembeck et al., 2006] (fig. 1). An increasing number of genes have been identified as targets of the β-catenin/TCF/LEF pathway. These include members of the matrix metalloproteinases (MMP), chemokines or cytoskeletal

KARGER
Fax +41 61 306 12 34
E-Mail karger@karger.ch
www.karger.com

1422–6405/07/1853–0061$23.50/0

Accessible online at:
www.karger.com/cto

Dr. Christine Gilles
Laboratory of Tumor and Developmental Biology, Liège University
CHU Sart-Tilman, Tour de Pathologie B23
BE–4000 Liège (Belgium)
Tel. +32 43 66 24 53, Fax +32 43 66 29 36, E-Mail cgilles@ulg.ac.be

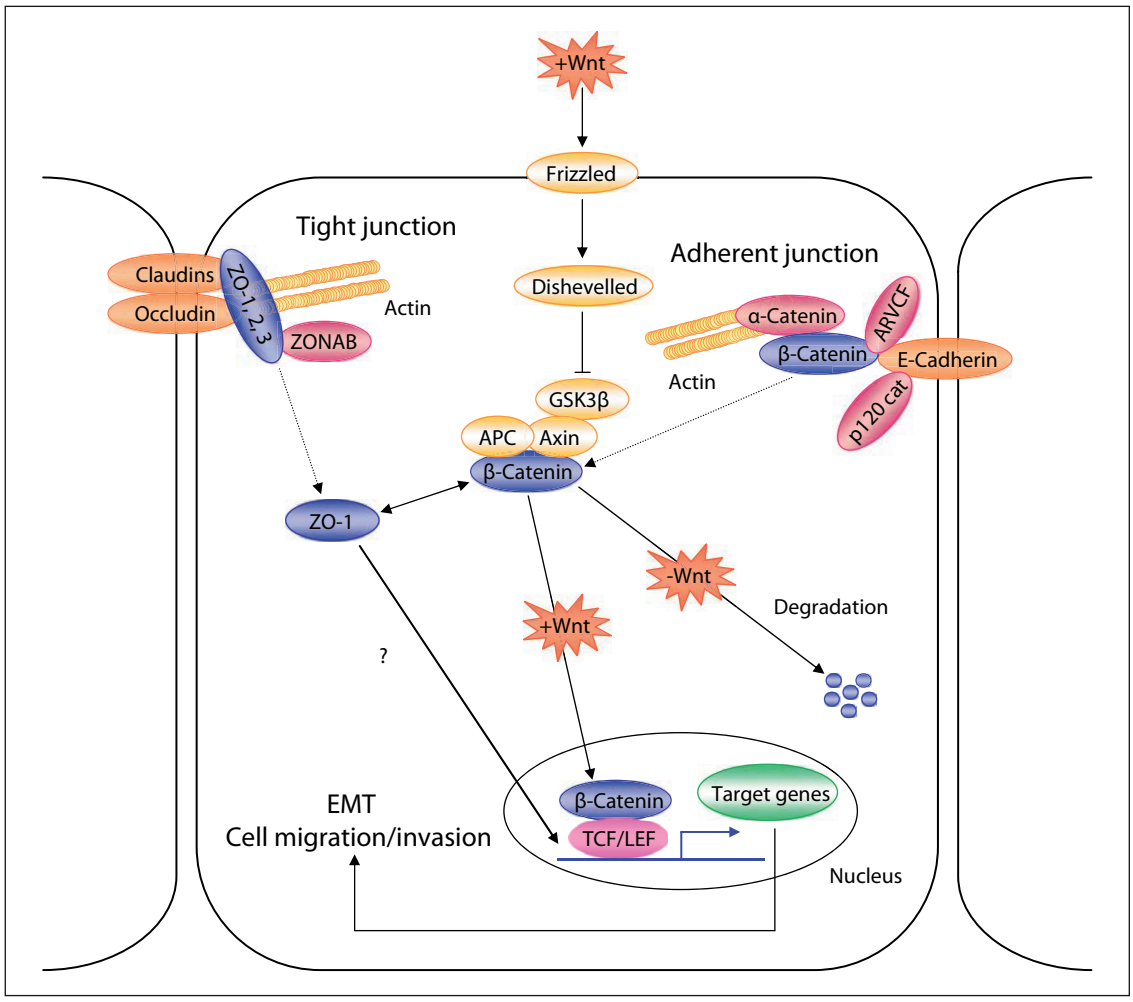

1

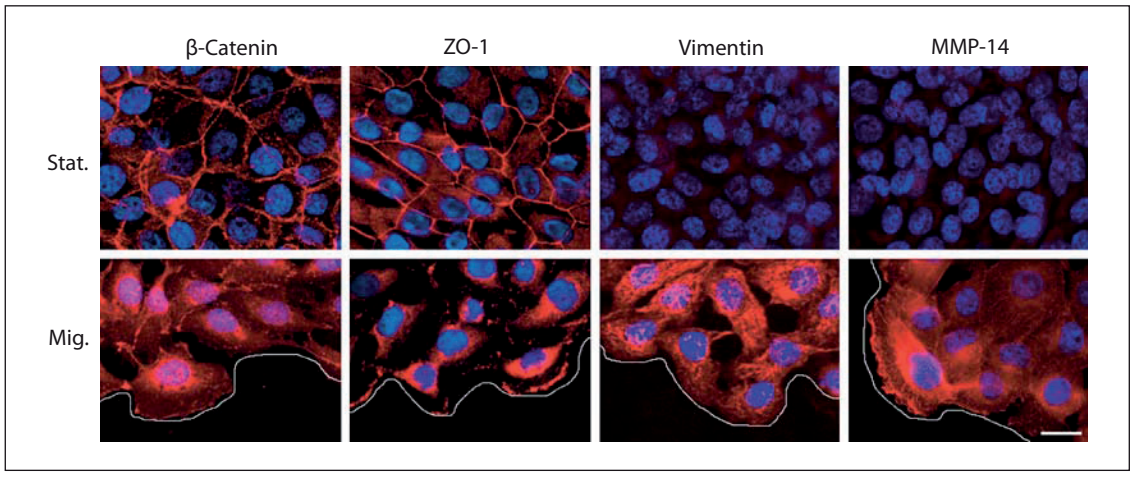

2

Fig. 1. Schematic representation of β-catenin and ZO-1 subcellular relocalization during EMT processes. In differentiated normal epithelial cells, both β-catenin and ZO-1 mostly localize at the cell-cell adhesion membrane complexes. During EMT, both β-catenin and ZO-1 relocalize from these membrane complexes, accumulate in the cytoplasm and eventually translocate to the nucleus. The activation of the Wnt pathway, inhibiting the degradation of the cytoplasmic β-catenin through the proteasome system, plays an important regulatory role in this scheme.

Fig. 2. Differential expression and localization of β-catenin, ZO-1, vimentin and MMP-14 in migratory versus stationary MCF10A human breast cells. MCF10A cells were seeded in growth medium

protein families, some of them having major implications in tumor progression [Brabletz et al., 1999; Marchenko et al., 2001; Levy et al., 2002; Takahashi et al., 2002; Gilles et al., 2003; Mestdagt et al., 2006]. Even though the implication of tight junction molecules in EMT is less well documented, a parallelism can nevertheless be depicted between the reorganization of adherens junctions and tight junctions occurring during EMT (fig. 1). Indeed, similar to adherens junctions, tight junctions comprise transmembrane molecules (occludin, claudins or junctional adhesion molecules/JAM) linked to the actin cytoskeleton through cytoplasmic linker molecules such as zonula occludens proteins (ZO) [Gonzalez-Mariscal et al., 2003]. A delocalization of ZO-1 from the cell membrane has been reported during epithelial cell migration and the presence of ZO-1 in the nuclei of migratory cells has also been observed [Gottardi et al., 1996]. Also, an interaction between ZO-1 and the transcriptional repressor ZONAB (ZO-1-associated nucleic acid-binding protein) has been demonstrated at the tight junctions. This results in the regulation of ZONAB nuclear levels and its subsequent ability to regulate gene expression [Balda and Matter, 2000; Balda et al., 2003]. Although the nuclear localization of ZO-1 remains controversial, both β-catenin and ZO-1 appear to be shuttle molecules. Depending upon the state of differentiation and migration of epithelial cells, β-catenin and ZO-1 may be found in different subcellular compartments and act as signaling proteins, regulating gene transcription. Although such shuttling properties have been assigned to several other adherens or tight junction molecular components [Balda and Matter, 2003], we will focus this summary on β-catenin and ZO-1 in tumor EMT systems.

inside a glass ring. Twenty-four hours after plating, the glass ring was removed and the cells at the periphery of the outgrowth initiated a directed migration from the confluent area initially delimited by the ring. Video microscopy measurements clearly identified a migratory (Mig.) subpopulation at the periphery of the outgrowth and a stationary subpopulation (Stat.) in the area initially delimited by the ring [Gilles et al., 1999]. In this assay, the migratory subpopulation clearly turned on vimentin and MMP-14 expression and displayed a rather cytoplasmic and/or nuclear staining for β-catenin and ZO-1. In contrast, the stationary subpopulation did neither express vimentin nor MMP-14 and displayed a membrane staining for both β-catenin and ZO-1. The white line schematically represents the migration front. β-Catenin, ZO-1, vimentin and MMP-14 immunostainings are in red. DAPI nuclear staining is in blue. Bar = 12 μm.

Because of their implication in gene regulation, we and others have investigated the potential roles of β-catenin and ZO-1 in upregulation of the mesenchymal gene expressions which is observed during the EMT processes associated with epithelial tumor cell invasion. Among the mesenchymal genes considered as good markers of EMT, there is vimentin. Vimentin is a type III intermediate filament which, in normal conditions in adults, is expressed by cells of mesenchymal origin [Steinert and Roop, 1988]. Accumulating evidence has now clearly shown that vimentin can also be expressed by migratory/invasive epithelial cells, and is functionally implicated in cell migration [Sommers et al., 1989, 1992, 1994b; Gilles et al., 1994b, 1996a, 1999, 2003; Hendrix et al., 1997; Singh et al., 2003]. Besides vimentin, several studies have also shown that MMP genes are turned on during EMT changes [Gilles et al., 2004]. MMPs are a family of proteases which cannot only degrade almost all ECM components, but also other key substrates such as cell-cell adhesion molecules, chemokines and cell surface receptors [Egeblad and Werb, 2002]. The consensus view is that many MMPs are, in general, mostly produced by stromal cells surrounding tumor cell clusters [Gilles et al., 2004; Polette et al., 2004]. However, expression of 'stromal' MMPs now appears as one of the major attributes that epithelial cells acquire after undergoing EMT processes [Gilles et al., 2004; Polette et al., 2004]. Among the MMP family, MMP-14 (MT1-MMP) and MMP-3 have been more particularly examined in relationship with EMT [Lochter et al., 1997; Pulyaeva et al., 1997; Sternlicht et al., 1999; Gilles et al., 2004]. If MMP-3 has been mostly studied as a potential inducer of EMT in mouse tumor cells, MMP-14, on which this summary is focused, has rather been looked at as a target gene of EMT events.

In summarizing data describing the expression and localization of β-catenin, ZO-1, vimentin and MMP-14 in different breast, cervical and lung cell lines displaying different degrees of invasiveness, a clear-cut correlation can be drawn. Indeed, noninvasive cell lines do not express vimentin or MMP-14 and mostly express β-catenin and ZO-1 at the membrane, whereas invasive cell lines express high levels of vimentin and MMP-14 and display a rather diffuse cytoplasmic and/or nuclear staining of β-catenin and ZO-1 [Sommers et al., 1989, 1992, 1194a; Thompson et al., 1992; Gilles et al., 1994a, b, 1996a, b; Pulyaeva et al., 1997; Polette et al., 1998]. These correlations have also been made using in vitro cell systems in which EMT can be induced. This is shown in figure 2, in a two-dimensional migration assay, using MCF10A human mammary epithelial cells. In this assay, one can ob-

serve that the migratory subpopulation undergoes an EMT characterized by the expression of vimentin and MMP-14 and a nuclear and/or cytoplasmic relocalization of β-catenin and ZO-1 [Gilles et al., 1999, 2001, 2003; Bindels et al., 2006]. In contrast, stationary cells neither express vimentin nor MMP-14, but show a typical epithelial honeycomb staining of β-catenin and ZO-1. In addition to these correlative data, we also showed that vimentin can be regulated by the β-catenin/TCF pathway in human breast tumor cells [Gilles et al., 2003]. Similarly, as also described for other MMPs, MMP-14 has been reported to be a target gene of the β-catenin/TCF pathway [Takahashi et al., 2002]. Regarding ZO-1, the transfection of the N-terminal fragment of ZO-1, which is unable to localize to the cell membrane, has been reported to induce EMT changes in MDCK cells characterized by an increased vimentin expression and enhanced invasiveness [Reichert et al., 2000]. We have also recently reported that transfection of ZO-1 siRNA downregulates MMP-14 mRNA and protein, subsequently decreasing the in vitro invasive abilities of human breast tumor cells [Polette et al., 2005]. Furthermore, both studies have demonstrated that an induction of the β-catenin/TCF/LEF pathway occurs following ZO-1 transfection, showing evidence of a cross talk between both pathways [Reichert et al., 2000; Polette et al., 2005].

In conclusion, during EMT, the loss of epithelial features can directly regulate the expression of mesenchymal genes. β-Catenin and ZO-1, which are a structural component of cell-cell adhesion complexes in differentiated epithelial cells, could each play a key role in such regulations through their ability to shuttle from the membrane to the cytosol or nucleus and act as signaling molecules.

Acknowledgments

This work was supported by grants from the CGRI-FNRS-INSERM coopération, the Lions Club of Soissons, the Fonds National de la Recherche Scientifique (FNRS, Belgium), the Fédération Belge Contre le Cancer and the Agency for Science, Technology and Research, Singapore.

References

Balda, M.S., K. Matter (2000) The tight junction protein ZO-1 and an interacting transcription factor regulate ErbB-2 expression. EMBO J *19:* 2024–2033.

Balda, M.S., M.D. Garrett, K. Matter (2003) The ZO-1-associated Y-box factor ZONAB regulates epithelial cell proliferation and cell density. J Cell Biol *160:* 423–432.

Balda, M.S., K. Matter (2003) Epithelial cell adhesion and the regulation of gene expression. Trends Cell Biol *13:* 310–318.

Bindels, S., M. Mestdagt, C. Vandewalle, N. Jacobs, L. Volders, A. Noel, F. van Roy, G. Berx, J.M. Foidart, C. Gilles (2006) Regulation of vimentin by SIP1 in human epithelial breast tumor cells. Oncogene *25:* 4975–4985.

Brabletz, T., A. Jung, S. Dag, F. Hlubek, T. Kirchner (1999) Beta-catenin regulates the expression of the matrix metalloproteinase-7 in human colorectal cancer. Am J Pathol *155:* 1033–1038.

Brembeck, F.H., M. Rosario, W. Birchmeier (2006) Balancing cell adhesion and Wnt signaling, the key role of beta-catenin. Curr Opin Genet Dev *16:* 51–59.

Egeblad, M., Z. Werb (2002) New functions for the matrix metalloproteinases in cancer progression. Nat Rev Cancer *2:* 161–174.

Gilles, C., J. Piette, W. Peter, N.E. Fusenig, J.M. Foidart (1994a) Differentiation ability and oncogenic potential of HPV-33 – and HPV-33+ ras-transfected keratinocytes. Int J Cancer *58:* 847–854.

Gilles, C., M. Polette, J. Piette, P. Birembaut, J.M. Foidart (1994b) Epithelial-to-mesenchymal transition in HPV-33-transfected cervical keratinocytes is associated with increased invasiveness and expression of gelatinase A. Int J Cancer *59:* 661–666.

Gilles, C., M. Polette, J. Piette, A.C. Delvigne, E.W. Thompson, J.M. Foidart, P. Birembaut (1996a) Vimentin expression in cervical carcinomas: association with invasive and migratory potential. J Pathol *180:* 175–180.

Gilles, C., M. Polette, J. Piette, C. Munaut, E.W. Thompson, P. Birembaut, J.M. Foidart (1996b) High level of MT-MMP expression is associated with invasiveness of cervical cancer cells. Int J Cancer *65:* 209–213.

Gilles, C., M. Polette, J.M. Zahm, J.M. Tournier, L. Volders, J.M. Foidart, P. Birembaut (1999) Vimentin contributes to human mammary epithelial cell migration. J Cell Sci *112:* 4615–4625.

Gilles, C., M. Polette, C. Coraux, J.M. Tournier, G. Meneguzzi, C. Munaut, L. Volders, P. Rousselle, P. Birembaut, J.M. Foidart (2001) Contribution of MT1-MMP and of human laminin-5 gamma2 chain degradation to mammary epithelial cell migration. J Cell Sci *114:* 2967–2976.

Gilles, C., M. Polette, M. Mestdagt, B. Nawrocki-Raby, P. Ruggeri, P. Birembaut, J.M. Foidart (2003) Transactivation of vimentin by beta-catenin in human breast cancer cells. Cancer Res *63:* 2658–2664.

Gilles, C., D. Newgreen, H. Sato, E.W. Thompson (2004) Matrix metalloproteases and epithelial-to-mesenchymal transition: implications for carcinoma metastasis; in Savagner, P. (ed): Rise and Fall of Epithelial Phenotype. Georgetown, Eurekah.com and Kluwer Academic/Plenum Publishers, chap 2.

Gonzalez-Mariscal, L., A. Betanzos, P. Nava, B.E. Jaramillo (2003) Tight junction proteins. Prog Biophys Mol Biol *81:* 1–44.

Gottardi, C.J., M. Arpin, A.S. Fanning, D. Louvard (1996) The junction-associated protein, zonula occludens-1, localizes to the nucleus before the maturation and during the remodeling of cell-cell contacts. Proc Natl Acad Sci USA *93:* 10779–10784.

Harris, T.J., M. Peifer (2005) Decisions, decisions: beta-catenin chooses between adhesion and transcription. Trends Cell Biol *15:* 234–237.

Hendrix, M.J., E.A. Seftor, R.E. Seftor, K.T. Trevor (1997) Experimental co-expression of vimentin and keratin intermediate filaments in human breast cancer cells results in phenotypic interconversion and increased invasive behavior. Am J Pathol *150:* 483–495.

Huber, M.A., N. Kraut, H. Beug (2005) Molecular requirements for epithelial-mesenchymal transition during tumor progression. Curr Opin Cell Biol *17:* 548–558.

Ikenouchi, J., M. Matsuda, M. Furuse, S. Tsukita (2003) Regulation of tight junctions during the epithelium-mesenchyme transition: direct repression of the gene expression of claudins/occludin by Snail. J Cell Sci *116:* 1959–1967.

Levy, L., C. Neuveut, C.A. Renard, P. Charneau, S. Branchereau, F. Gauthier, J.T. Van Nhieu, D. Cherqui, A.F. Petit-Bertron, D. Mathieu, M.A. Buendia (2002) Transcriptional activation of interleukin-8 by beta-catenin-Tcf4. J Biol Chem *277:* 42386–42393.

Lochter, A., S. Galosy, J. Muschler, N. Freedman, Z. Werb, M.J. Bissell (1997) Matrix metalloproteinase stromelysin-1 triggers a cascade of molecular alterations that leads to stable epithelial-to-mesenchymal conversion and a premalignant phenotype in mammary epithelial cells. J Cell Biol *139:* 1861–1872.

Marchenko, G.N., B.I. Ratnikov, D.V. Rozanov, A. Godzik, E.I. Deryugina, A.Y. Strongin (2001) Characterization of matrix metalloproteinase-26, a novel metalloproteinase widely expressed in cancer cells of epithelial origin. Biochem J *356:* 705–718.

Mestdagt, M., M. Polette, G. Buttice, A. Noel, A. Ueda, J.M. Foidart, C. Gilles (2006) Transactivation of MCP-1/CCL2 by beta-catenin/TCF-4 in human breast cancer cells. Int J Cancer *118:* 35–42.

Polette, M., C. Gilles, S. de Bentzmann, D. Gruenert, J.M. Tournier, P. Birembaut (1998) Association of fibroblastoid features with the invasive phenotype in human bronchial cancer cell lines. Clin Exp Metastasis *16:* 105–112.

Polette, M., B. Nawrocki-Raby, C. Gilles, C. Clavel, P. Birembaut (2004) Tumour invasion and matrix metalloproteinases. Crit Rev Oncol Hematol *49:* 179–186.

Polette, M., C. Gilles, B. Nawrocki-Raby, J. Lohi, W. Hunziker, J.M. Foidart, P. Birembaut (2005) Membrane-type 1 matrix metalloproteinase expression is regulated by zonula occludens-1 in human breast cancer cells. Cancer Res *65:* 7691–7698.

Pulyaeva, H., J. Bueno, M. Polette, P. Birembaut, H. Sato, M. Seiki, E.W. Thompson (1997) MT1-MMP correlates with MMP-2 activation potential seen after epithelial to mesenchymal transition in human breast carcinoma cells. Clin Exp Metastasis *15:* 111–120.

Reichert, M., T. Muller, W. Hunziker (2000) The PDZ domains of zonula occludens-1 induce an epithelial to mesenchymal transition of Madin-Darby canine kidney I cells. Evidence for a role of beta-catenin/Tcf/Lef signaling. J Biol Chem *275:* 9492–9500.

Singh, S., S. Sadacharan, S. Su, A. Belldegrun, S. Persad, G. Singh (2003) Overexpression of vimentin: role in the invasive phenotype in an androgen-independent model of prostate cancer. Cancer Res *63:* 2306–2311.

Sommers, C.L., D. Walker-Jones, S.E. Heckford, P. Worland, E. Valverius, R. Clark, F. McCormick, M. Stampfer, S. Abularach, E.P. Gelmann (1989) Vimentin rather than keratin expression in some hormone-independent breast cancer cell lines and in oncogene-transformed mammary epithelial cells. Cancer Res *49:* 4258–4263.

Sommers, C.L., S.E. Heckford, J.M. Skerker, P. Worland, J.A. Torri, E.W. Thompson, S.W. Byers, E.P. Gelmann (1992) Loss of epithelial markers and acquisition of vimentin expression in adriamycin- and vinblastine-resistant human breast cancer cell lines. Cancer Res *52:* 5190–5197.

Sommers, C.L., S.W. Byers, E.W. Thompson, J.A. Torri, E.P. Gelmann (1994a) Differentiation state and invasiveness of human breast cancer cell lines. Breast Cancer Res Treat *31:* 325–335.

Sommers, C.L., J.M. Skerker, S.A. Chrysogelos, M. Bosseler, E.P. Gelmann (1994b) Regulation of vimentin gene transcription in human breast cancer cell lines. Cell Growth Differ *5:* 839–846.

Steinert, P.M., D.R. Roop (1988) Molecular and cellular biology of intermediate filaments. Annu Rev Biochem *57:* 593–625.

Sternlicht, M.D., A. Lochter, C.J. Sympson, B. Huey, J.P. Rougier, J.W. Gray, D. Pinkel, M.J. Bissell, Z. Werb (1999) The stromal proteinase MMP3/stromelysin-1 promotes mammary carcinogenesis. Cell *98:* 137–146.

Takahashi, M., T. Tsunoda, M. Seiki, Y. Nakamura, Y. Furukawa (2002) Identification of membrane-type matrix metalloproteinase-1 as a target of the beta-catenin/Tcf4 complex in human colorectal cancers. Oncogene *21:* 5861–5867.

Thiery, J.P. (2003) Epithelial-mesenchymal transitions in development and pathologies. Curr Opin Cell Biol *15:* 740–746.

Thompson, E.W., S. Paik, N. Brunner, C.L. Sommers, G. Zugmaier, R. Clarke, T.B. Shima, J. Torri, S. Donahue, M.E. Lippman (1992) Association of increased basement membrane invasiveness with absence of estrogen receptor and expression of vimentin in human breast cancer cell lines. J Cell Physiol *150:* 534–544.

Wheelock, M.J., K.R. Johnson (2003) Cadherins as modulators of cellular phenotype. Annu Rev Cell Dev Biol *19:* 207–235.

Annexe 2 : Matériels et Méthodes

I. Génération de modèles cellulaires exprimant la luciférase et SIP1

Plasmides :

Le plasmide pcDNA3-Luc contient l'ADNc de la luciférase cloné en aval du promoteur CMV (cytomégalovirus) et permet une sélection à la généticine (G418, Life Technologies, Grand Island, NY).

Le plasmide pEF6-myc/his-SIP1 contient l'ADNc de SIP1 cloné en aval du promoteur CMV et permet une sélection à la blasticidine (Invitrogen Corporation, Scotland). Ce plasmide nous a été généreusement fourni par le Docteur Geert Berx (Université de Ghent).

Transfection stable par électroporation :

$4x10^6$ cellules BT20 sont resuspendues dans 800µl de DMEM sans sérum et placées dans une cuvette d'électroporation (Bio Rad Laboratories, Hercules, CA) en présence de 8µg de plasmides. La cuvette est ensuite placée dans l'appareil à électroporation (Gene Pulser, (Bio-Rad Laboratories, Hercules, CA) et les cellules sont soumises à un choc électrique (paramètres : 250 Volts, 950 µF). Les cellules ainsi transfectées sont ensuite placées dans un disque de culture en présence de milieu de culture complet (DMEM additionné de 10% de sérum de veau fœtal). 48h après transfection, les cellules sont soumises à une pression de sélection pendant 3 semaines avec l'antibiotique adéquat (généticine à 125 µg/ml ; blasticidine à 25 µg/ml).

Afin de générer les lignées exprimant SIP1 et la luciférase, nous avons procédé en deux étapes. Dans un premier temps, les cellules ont été transfectées avec le plasmide pcDNA3-Luc. Après une sélection de trois semaines en généticine, plusieurs clones ont été isolés grâce à des anneaux de clonage. Un clone exprimant fortement la luciférase a été sélectionné après lecture à l'IVIS 200. Pour ce faire les cellules sont incubées 10 minutes en présence de luciférine (150 µg/ml) et visualisées avec l'IVIS 200 avec des temps d'exposition variant de 5 à 30 secondes

Ce clone exprimant fortement la luciférase a été transfecté ensuite avec pEF6-myc/his-SIP1 ou le plasmide « vide » comme contrôle. Après une sélection de 3 semaines en blasticidine, deux populations cellulaires ont été générées : une population exprimant SIP1 et une population contrôle de cellules transfectées avec le vecteur « vide ».

II. Injection des cellules tumorales en souris

Les cellules tumorales mammaires BT20 transfectées stablement avec le plasmide SIP1 ou le vecteur contrôle sont resuspendues à une densité de 4.10^6 cellules/200µl de milieu DMEM sans additifs. Du matrigel (12,5 mg/ml) est ajouté à la suspension cellulaire en proportion 1:1 et 400µl du mélange est injecté en sous-cutanée dans chacun des flancs de souris immunodéficientes âgées de 6 semaines.

La lignée de mélanomes B16F10 transfectée transitoirement avec les siRNA SIP1 murins ou siRNA contrôles sont resuspendues à une densité de 200.000 cellules/200µl de milieu DMEM sans additifs. Cette suspension est injectée en sous-cutanée dans chacun des flancs de souris C57 Bl/6 âgées de 6 semaines.

III. Analyse de la croissance tumorale

La taille des tumeurs est répertoriée régulièrement en mesurant leur longueur et leur largeur. Le volume des tumeurs est alors déterminé en appliquant la formule : $l^2 \times L^2 \times \pi/6$ (Reichert et al., 2000).

VI. Analyse du potentiel métastatique avec l'appareil d'imagerie sur petits animaux (IVIS 200, Xenogen, Caliper)

1) *In toto* :

La formation de métastases a été évaluée en visualisant les souris *in toto* vivantes périodiquement sur l'appareil d'imagerie. Pour ce faire, les souris subissent une anesthésie gazeuse à l'isoflurane (2,5%). Elles sont injectées de manière intrapéritonéale avec 100µl d'une solution de PBS contenant la luciférine, substrat de la luciférase (30 mg/ml). 12 minutes après l'injection de la luciférine, elles sont alors placées sur la plateforme de l'appareil, toujours sous anesthésie, pendant une période variant de 20 secondes à 1 minute d'exposition nécessaire à la détection du signal chémiluminescent émis par les cellules et à la prise d'image. La présence de signaux dits « internes » en dehors des signaux correspondant aux tumeurs primaires atteste de la présence potentielle de métastases.

2) Après dissection :

Lorsque des « signaux internes » sont visualisés *in toto,* les souris sont sacrifiées et les organes disséqués et analysés sur l'appareil d'imagerie. La quantification du potentiel métastatique est réalisée en attribuant un score correspondant à l'intensité de luminescence lue pour chaque organe.

Les tumeurs sous-cutanées et certains organes (poumon, rein, rate, foie, ovaires, intestins) sont alors prélevés et enchâssés en paraffine pour des analyses histologiques.